# Astrophysics C1
# Advanced stellar astrophysics and galaxies
# Lecture 7

**Michele Cappellari**

UNIVERSITY OF OXFORD

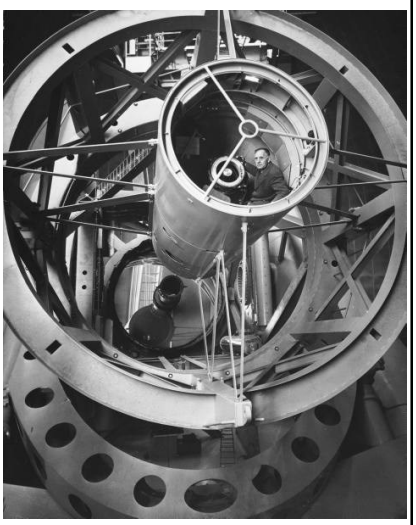
1

## Part II
## Galaxy Structure
## Dynamics and Formation

2

# Historical overview 1

- Astrophysics progress closely linked to that of instrumentation
- **1930:** Photographic plates: good morphology
- **1975:** Image intensifiers: Kinematics of ellipticals
- **1985:** CCD photometry from the ground
  - Deviations of isophotes from ellipses
  - Density constant in the center
- **1990:** Photometry with HST
  - Density rises until smallest observable radii (<0.05")
  - Density cusp/cores.

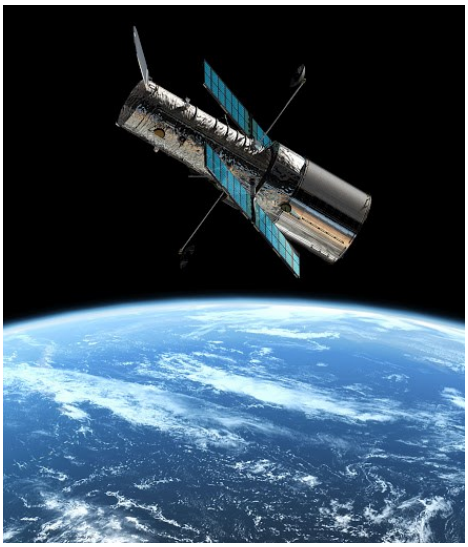


Hubble on the 5m Palomar Telescope

3

# Historical overview 2

- **1995:** slit spectroscopy with HST
  - Steep rise in central velocity and dispersion
  - Supermassive black holes!
- **2000:** Integral-field spectroscopy (IFS). Velocity fields.
- **2005:** Integral-field spectroscopy with adaptive optics
- **2013-** Multi-IFS surveys



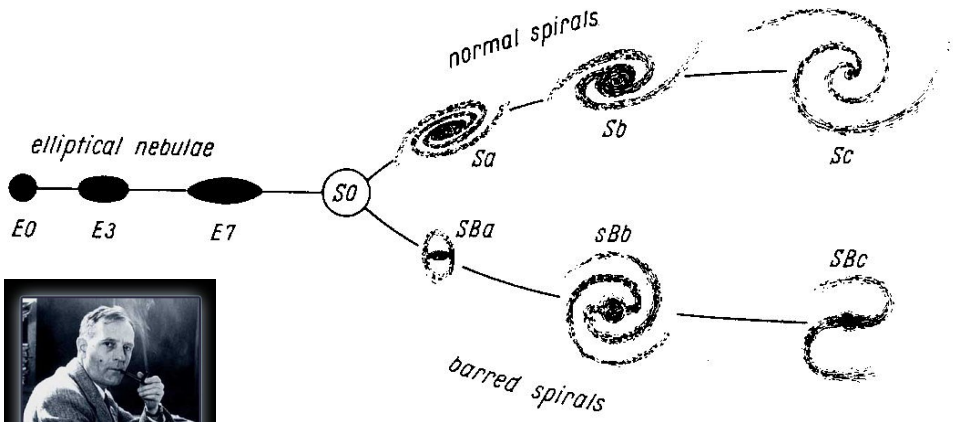
Hubble Space Telescope (image credit ESA)

4

# Galaxy Morphology

5

## Galaxy classification: 1936



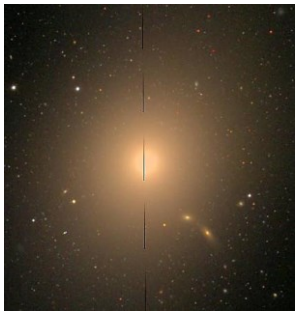



Edwin Hubble (1889-1953)

"S0" proposed as a "hypothetical" class
Hubble (1936, *Realm of Nebulae*)

6

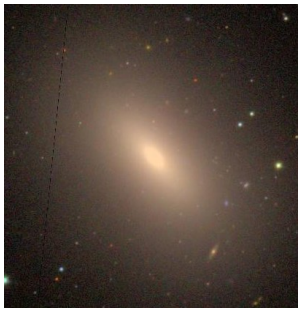
# Elliptical galaxies



M87 (E0)



M89 (E0)

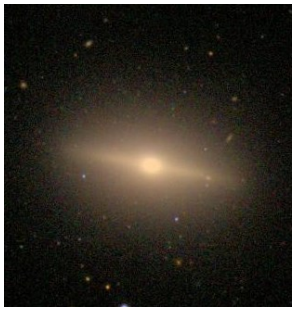


NGC3377 (E5)

- Featureless
- Mostly round
- No disks

7

# Lenticular galaxies



NGC4474 (S0)



NGC4477 (SB0)



NGC3156 (S0)

- Can be flattened
- Disks but no spiral arms
- Often bars

8

# Spiral galaxies

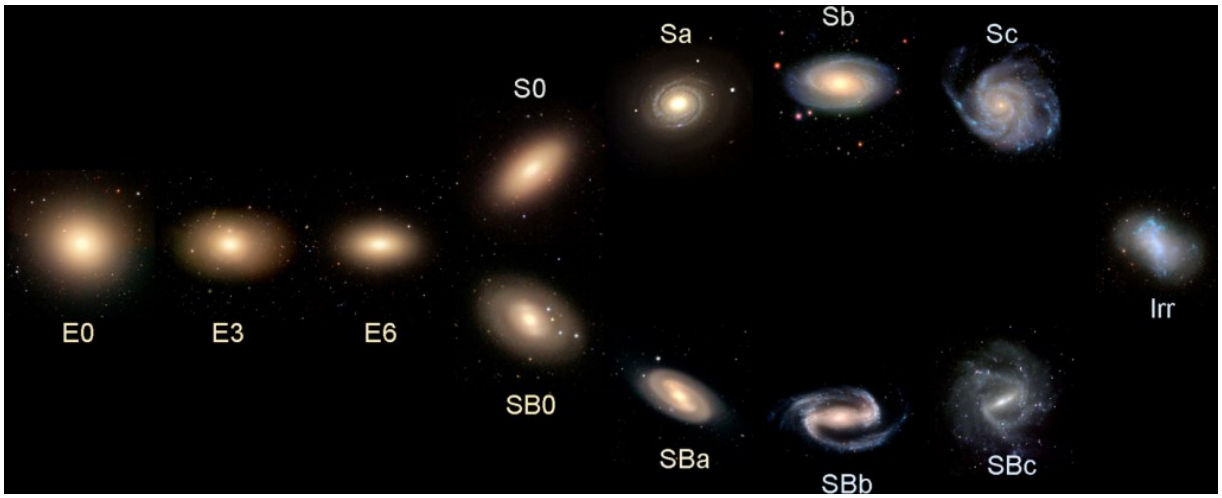


M65 (Sa) M88 (Sb) M51 (Sc)

- Disks with dusty spiral arms
- Bulge fraction related to spiral arms structure
- Star formation (blue color)

9

# Modern view of Hubble diagram




By John Kormendy

10

# Stellar light distribution

11

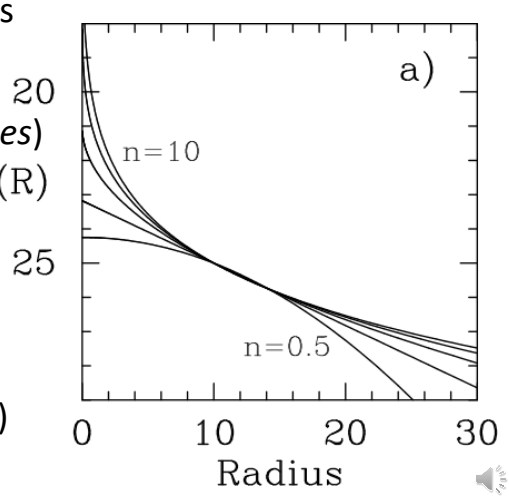
## Global galaxy profiles

- Empirical description of surface brightness
- $\Sigma(r) = \Sigma_0 \exp\left[-b_n (r/r_e)^{\frac{1}{n}}\right]$

Serisc `law' (1968, *Atlas de galaxias australes*)

- n → concentration
- $r_e$ → effective radius

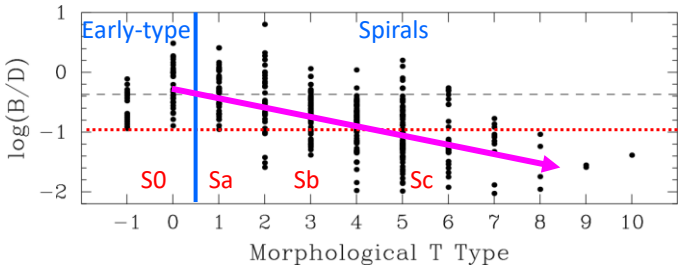
- Generally, two-components
- Bulge: n = 4 → de Vaucouleurs (1948)
- Disk: n = 1 → exponential (Freeman 1970)



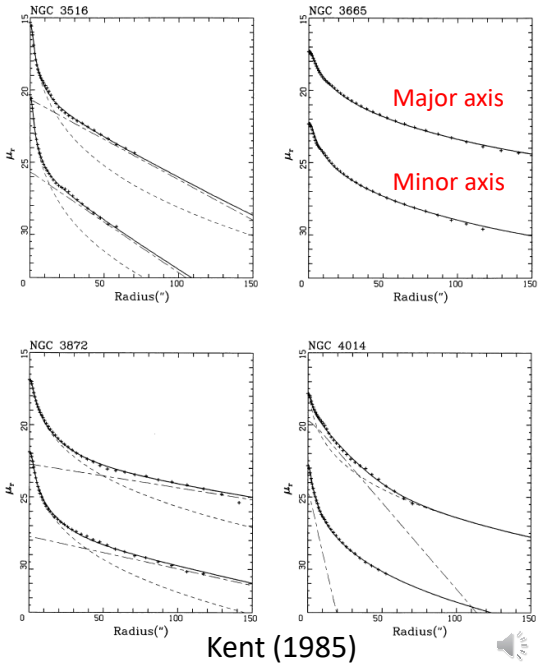

12

# Bulge ratio vs Hubble type

- exp(-k $r^{1/4}$) near the center
- exp(-k r) at large radii
- B/D → bulge over disk light
- Hubble sequence → trend in B/T with mass



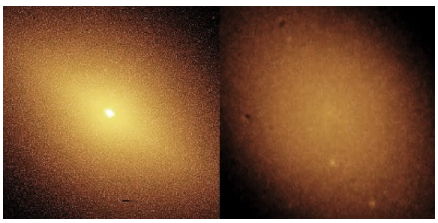

Graham & Worley (2008)



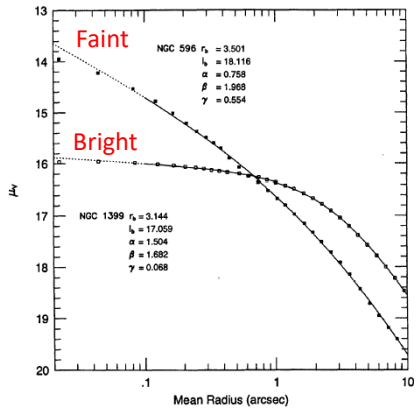

Kent (1985)

13

# Nuclear galaxy profiles



Lauer et al. (2005)



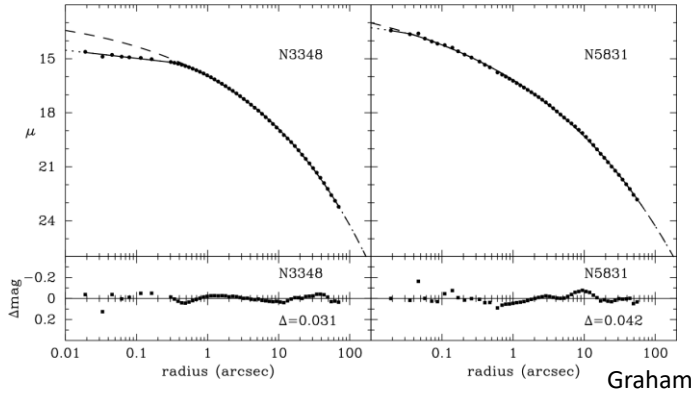

Lauer et al. 1995

- Fit double power-law to HST images
- Bright ellipticals: break in profile
- Faint ellipticals: single power-law

(Jaffe et al. 1994; Lauer et al. 1995; Faber et al. 1997)

14

# Central light deficit

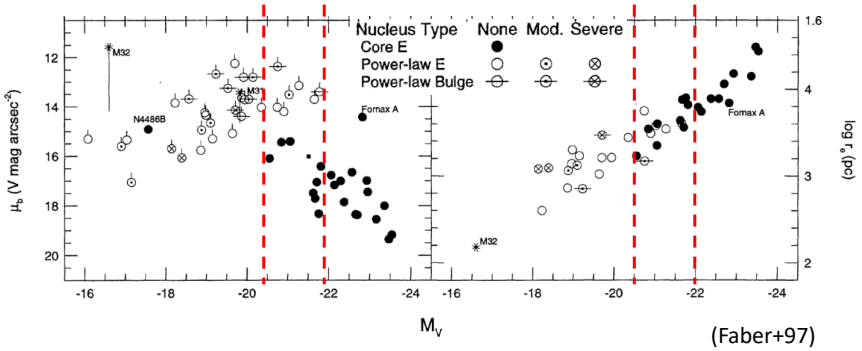



Graham (2003)

- Fit global profile to the whole galaxy
- Profile Break → deficit versus Sersic
- Power-law galaxies = pure Sersic profiles

15

# Nuclear profiles and luminosity



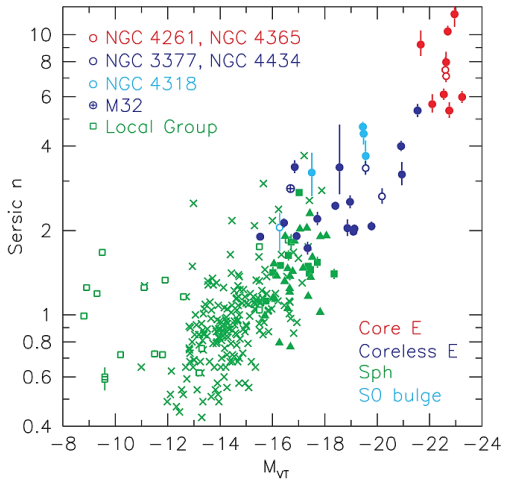

(Faber+97)

- Core/deficit dominate for $M_V < -22$
- Core-cusp overlap $-22 < M_V < -20.5$

16

# Global profiles and luminosity

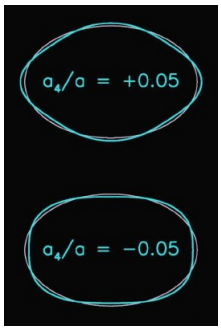
- Larger Sersic-*n* for luminous galaxies (Caon+93)
- Bright galaxies more concentrated
- $n \sim 1$ → exponential for faint galaxies
- Faint galaxies are disk-like

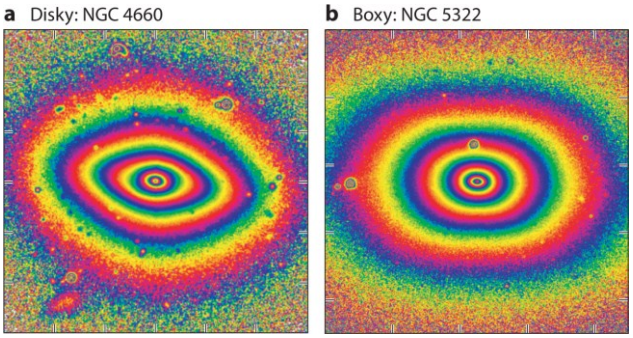



Kormendy+09

17

# Isophotal shape



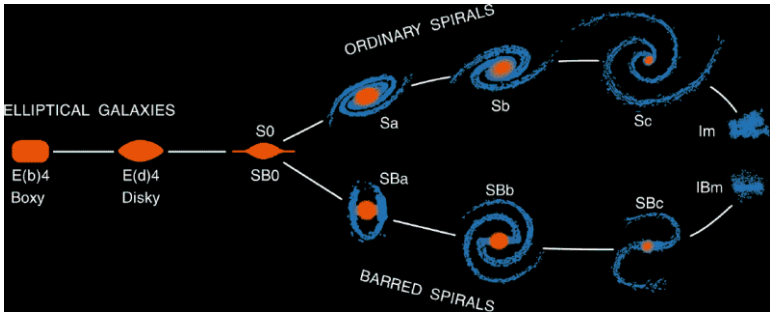

Cappellari (2016 ARA&A)

- Ellipticals can have disky or boxy isophotes
  - Bright ellipticals: boxy
  - Faint ellipticals: disky
- Disky isophotes = elliptical isophote + faint disk

(Bender 1988; Bender et al. 1989)

18

# Galaxy classification: 1996




(Kormendy+Bender96)

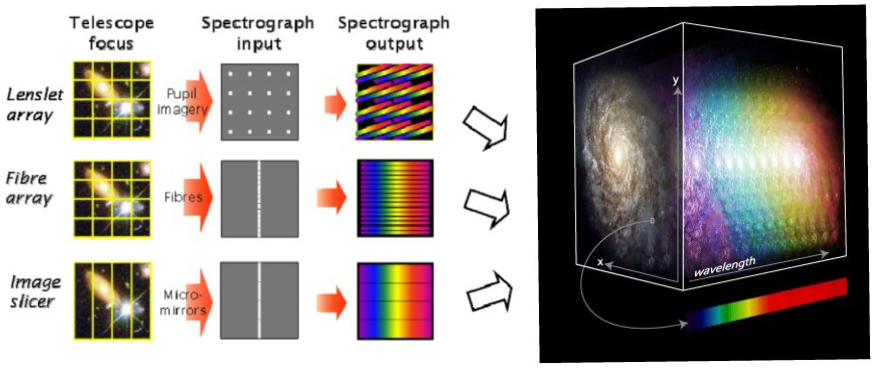
- Statistics: many inclined E may contain disks
  (Rix+White90; vanDenBergh90; Jorgensen+Franx94; Michard94)
- Disky ellipticals: transition between bright E and S0
  (Kormendy+Bender96)

19

# Modelling stellar population of external galaxies

20

# Integral-field spectroscopy



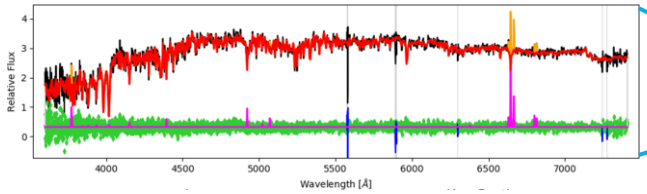

(Allington-Smith 2006)

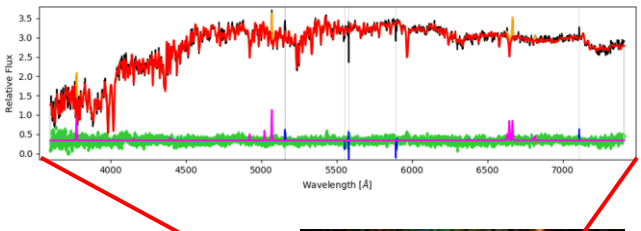
- Integral-field spectroscopy
- Various technical approaches
- All produce a three-dimensional data-cube

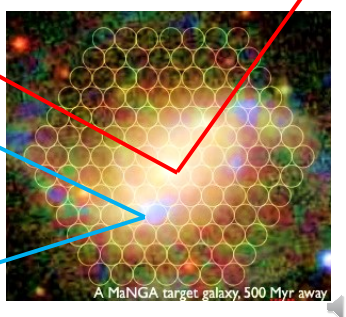
21

# What we can observe for external galaxies

- Best information provided by integral-field spectroscopy
- Gives one spectrum at every spatial position on galaxies
- How can we extract stellar population from spectra?



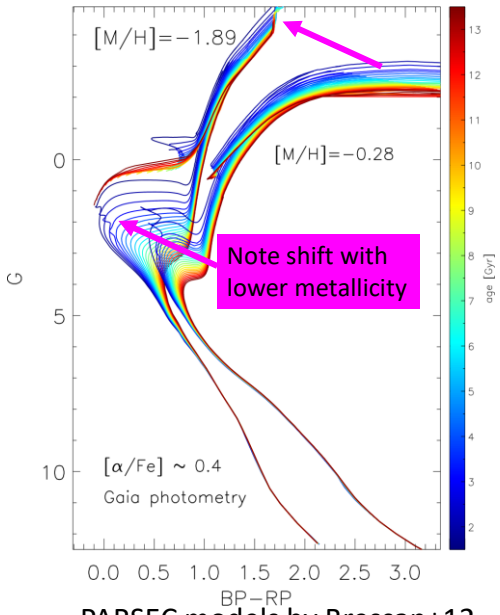




22

# State-of-the-art models

- Decades of progress in stellar evolution
- Extensive databases of opacities calculation, nuclear reactions rates, and atomic lines
- Includes various empirical calibration
- Approximate criteria for convective zones
- Numerical solution of differential equations
- Complex codes producing detailed isochrones as a function of key parameters
  - Age T
  - Metallicity $[\mathrm{Fe/H}]$
  - Alpha elements enhancement $[\alpha/\mathrm{Fe}]$

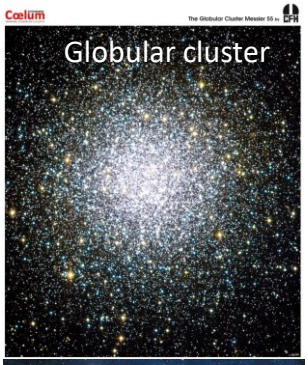


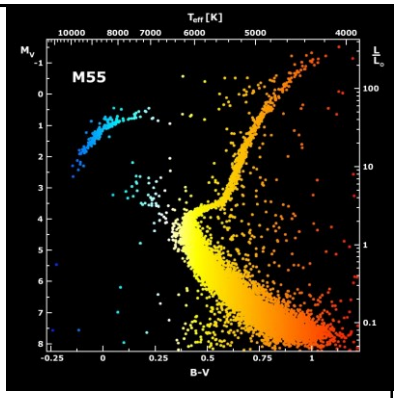

PARSEC models by Bressan+12
(Figure from Xiaoting Fu+17)

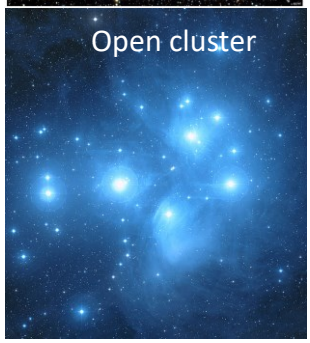
23

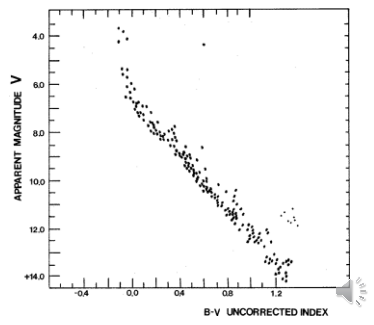
# Clusters HR diagrams

- Stars in stellar clusters are at same distance
- Relative distance errors disappear
- Stars formed at the same time
- HR diagrams for clusters empirically show stellar isochrones



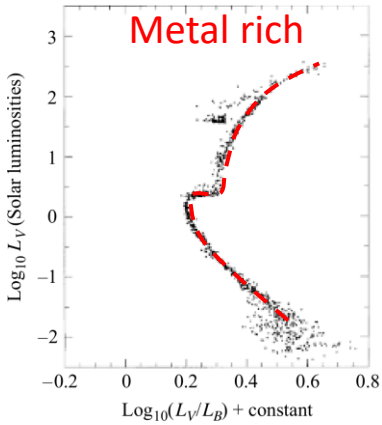



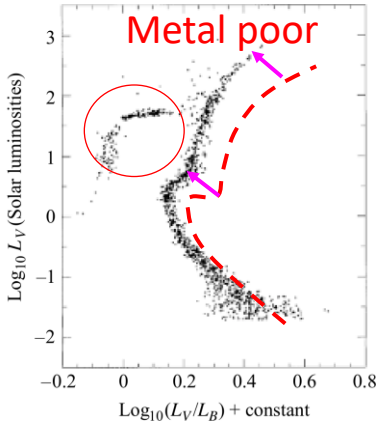

24

# H-R diagram changes with metallicity

- Metal lines absorb flux from V-band continuum
- Energy re-emitted at lower energy (longer wavelength)
- Metals also increase $H^-$
- This increases opacity
- → We see less deep into the stellar atmosphere
- Both (i) re-emission and (ii) opacity effects mimic a temperature increase
- Also metal-poor horizontal branch much more extended




47 Tuc Hesser+1987

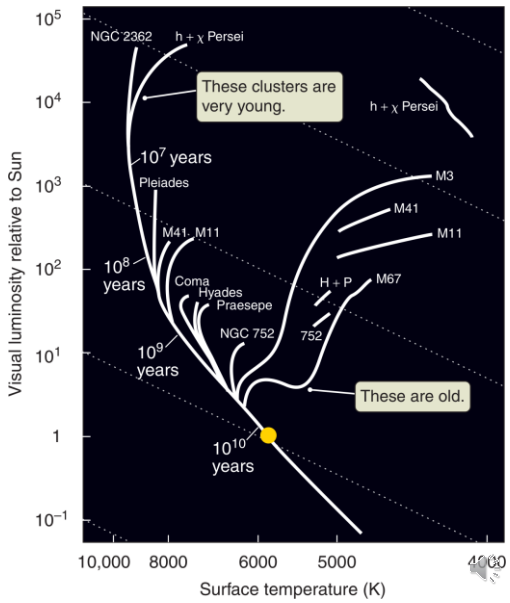



M15 Durrell & Harris 1993

25

# Ages from H-R diagrams of stellar clusters

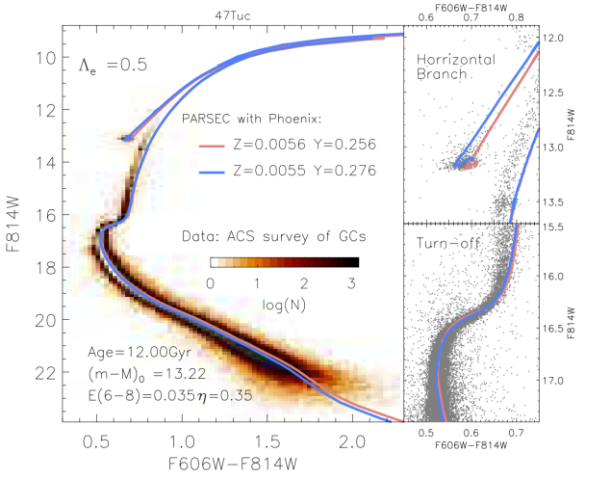
- Extent of main sequence (MS) is an obvious indication of age
- Young open clusters have extended MS
- Old globular clusters show giant branch
- But real observations do not give temperatures and ages directly
- We only observe magnitudes




26

# Stellar isochrone fitting

- Isochrones can be fitted to colour-magnitude diagrams
- One needs stellar spectra to convert isochrones to colours
- Effect of interstellar extinction needs to be included
- Fitting as a function of
  - Age T
  - Metallicity $[\mathrm{Fe/H}]$
  - Alpha elements enhancement $[\alpha/\mathrm{Fe}]$
- Stellar clusters are key benchmark for stellar evolution codes




Xiaoting Fu+18

27

# Single stellar population (SSP) models

Stellar spectra

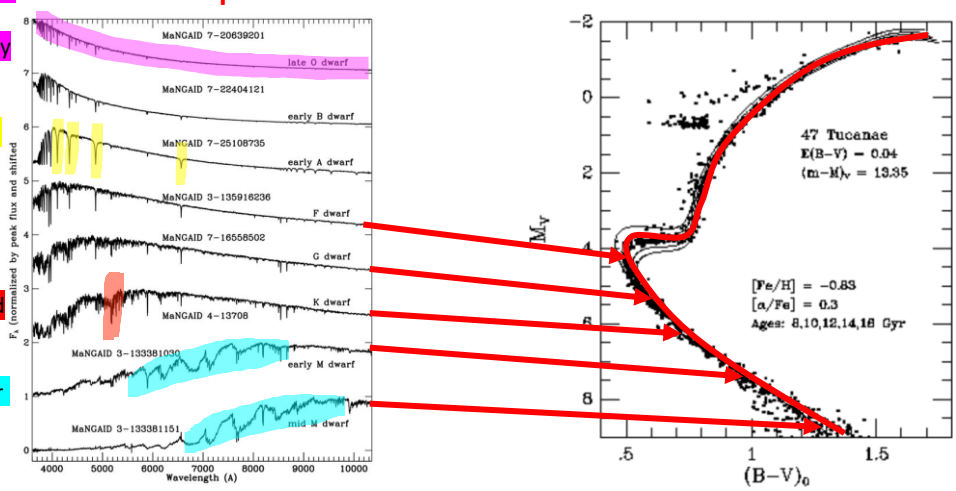
Isochrones

Featureless almost black body

H Balmer series

Mgb band

Broad molecular bands

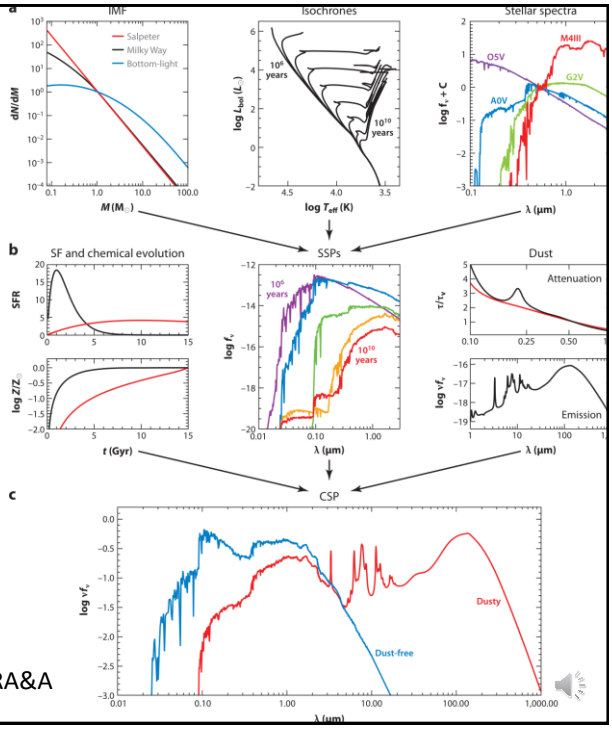



- Two basic ingredients are stellar spectra (synthetic or empirical) and model isochrones
- The resulting model spectrum is the weighted sum of all spectra along isochrone

28

# Single stellar population (SSP) model spectra

- SSP is building block for studying galaxies stellar population
- Requires assumption on stellar initial mass function
- Requires choice of elemental abundances
- May include modelling of photons reprocessing by dust and gas

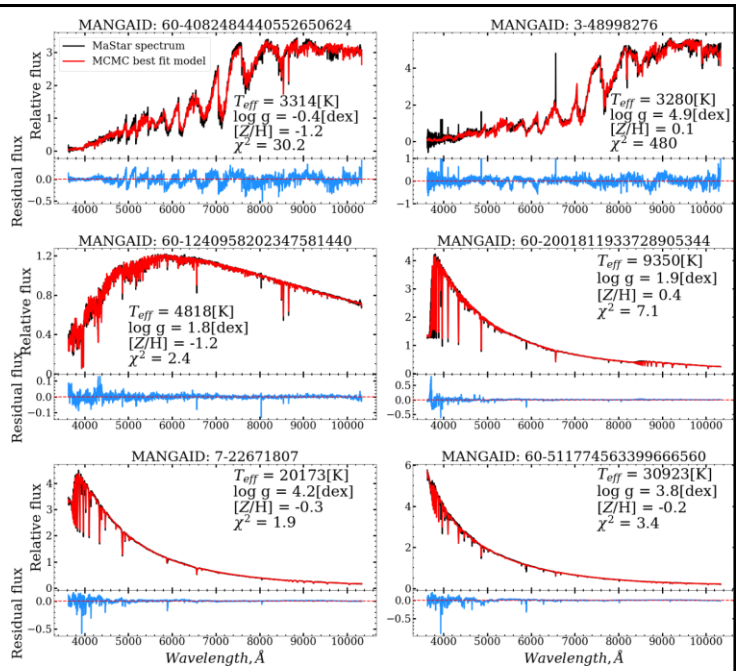



Conroy 2013 ARA&A

29

# Measuring key stellar parameters

- Very high resolution is needed for detailed elemental abundances
- But key parameters are $T_{\rm eff}, \log g, [Z/H]$
- Can be extracted efficiently for many stars
- Largest stellar library MaStar has 10,000 stars (Yan+19)

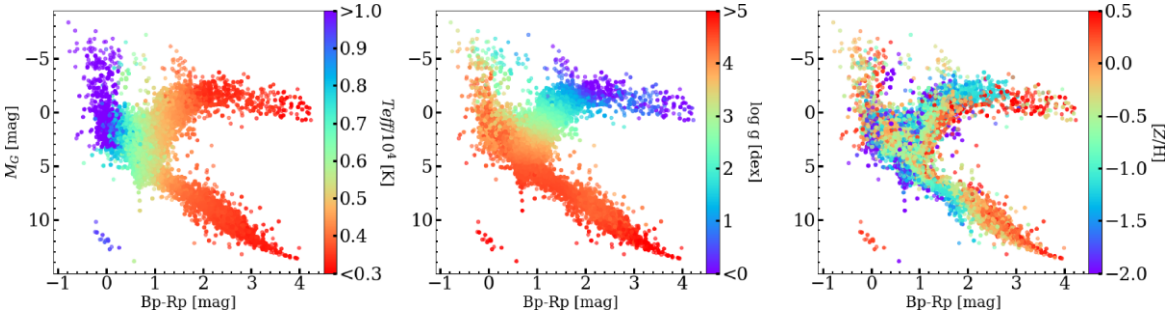



Hill+20 from MaNGA survey

30

# H-R diagram with Gaia distances

Hill+20 from MaNGA survey

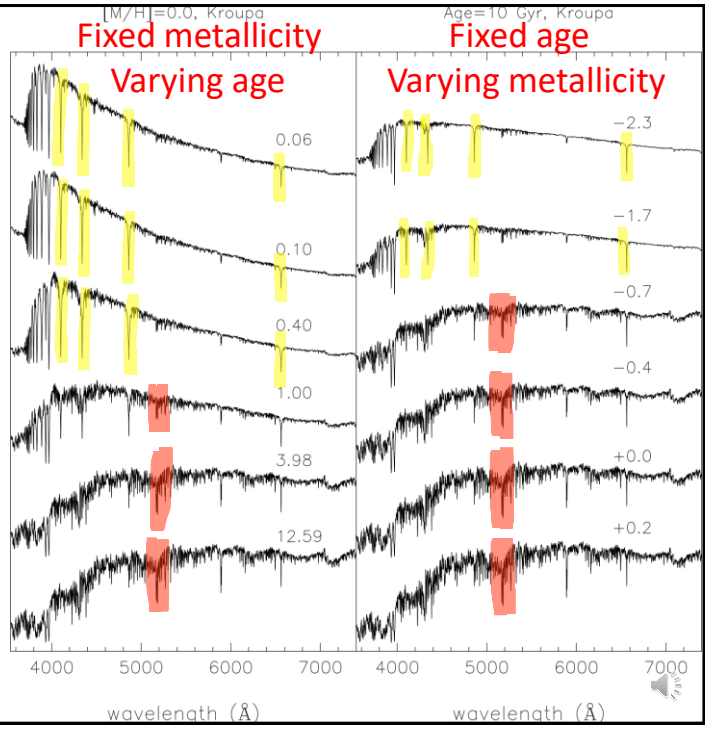



- Obtained with spectral fitting of synthetic models
- Recovers expected temperature and gravity trends
- Add metallicity dependence

31

# Age-metallicity degeneracy

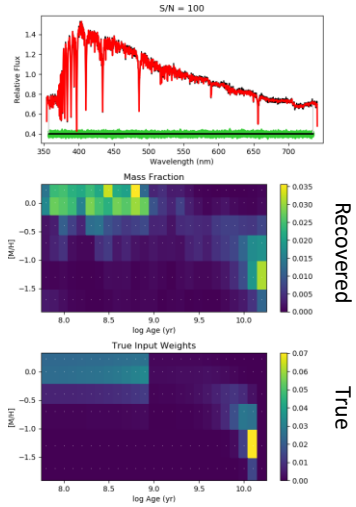
- Spectrum of a population of given age is dominated in visual region by stars at top of main sequence
- Dominated by Balmer lines for $t \lesssim 1Gyr$
- Dominated by metal bands at older ages
- Lowering metallicity is similar to lowering age (analogue to the effect on H-R diagram)




32

# Extracting stellar population in galaxies

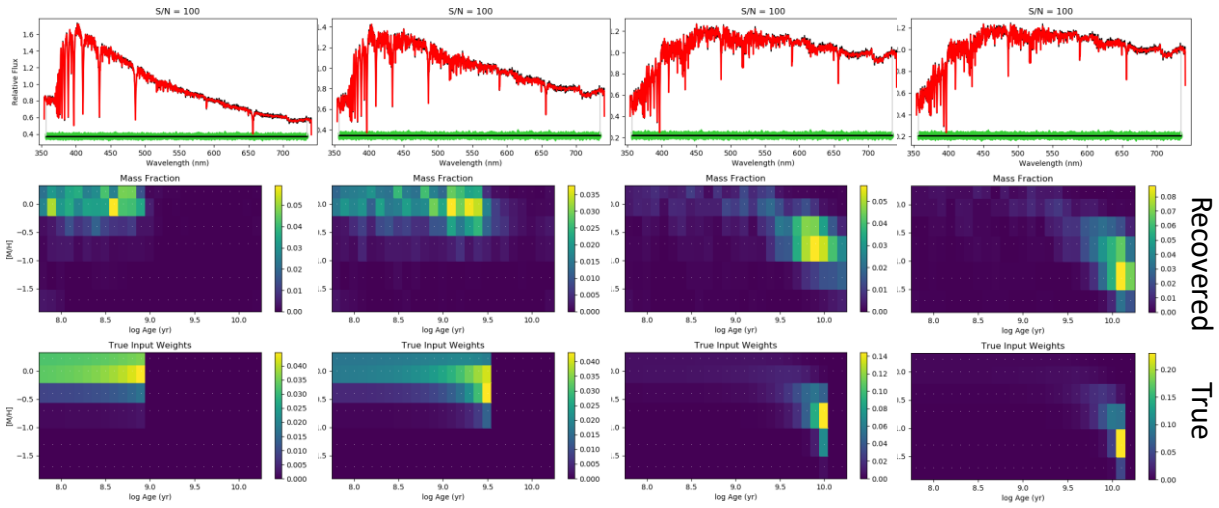
- Let's assume we study the distribution of ages in a galaxy
- Observed galaxy spectrum can be described by
- $G_{mod}(\lambda) = \int_{t=0}^{t=T} \mathrm{SFR}(T-t)\mathrm{SSP}_{\lambda}\,(t,[\mathrm{Fe}/H])dt$
- This integral can be discretized as
- $G_{\mathrm{mod}}(\lambda) = \sum_{n=1}^{N} w_n \mathrm{SSP}_n(\lambda)$ with $w_n \geq 0$
- Where $\mathrm{SSP}_n(\lambda)$ span a grid of ages $t = 0, \ldots, T$
- In general, one can study multiple parameters e.g., $(t, [\mathrm{Fe}/H], [\alpha/\mathrm{Fe}])$
- Solution is a quadratic problem for which formally unique solution and efficient algorithm exist
- But the problem is Fredholm equation of first kind
- Textbook example of ill-conditioned inverse problem
- Straightforward solution is not meaningful
- Techniques for ill-conditioned problem should be used




Fitting with pPXF
Cappellari (2017)

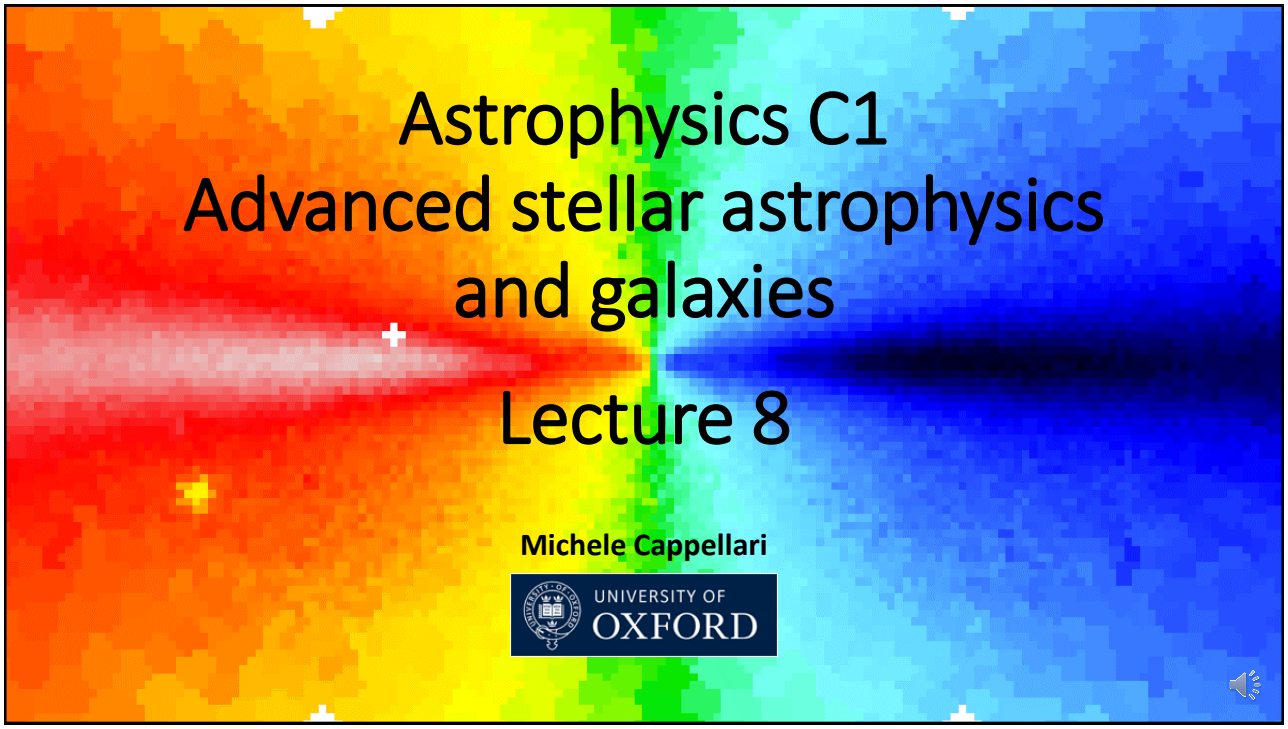
33

# Examples of stellar population extraction




Fitting with pPXF Cappellari (2017)

34

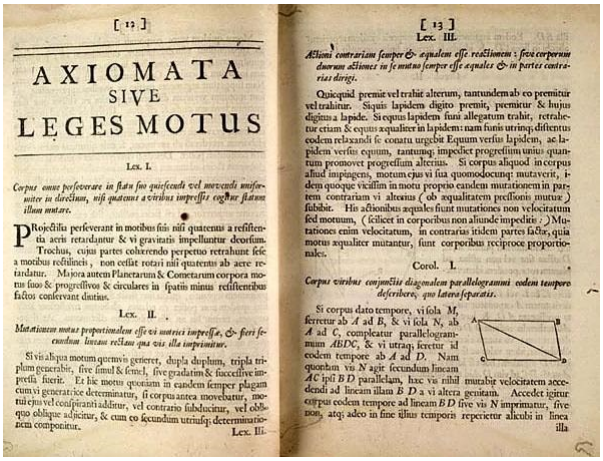



1

# Galactic Dynamics

2

# Isaac Newton 1643-1727



AXIOMATA
SIVE
LEGES MOTUS

Lex. I.

*Corpus omne perseverare in statu suo quiescendi vel movendi uniformiter in directum, nisi quatenus a viribus impressis cogitur statum illum mutare.*

Projectilia perseverant in motibus suis nisi quatenus a resistentia aeris retardantur & vi gravitatis impelluntur deorsum. Trochus, cujus partes cohærendo perpetuo retrahunt sese a motibus rectilineis, non cessat rotari nisi quatenus ab aere retardatur. Majora autem Planetarum & Cometarum corpora motus suos & progressivos & circulares in spatiis minus resistentibus factos conservant diutius.

Lex. II.

*Mutationem motus proportionalem esse vi motrici impressæ, & fieri secundum lineam rectam qua vis illa imprimitur.*

Si vis aliqua motum quemvis generet, dupla duplum, tripla triplum generabit, sive simul & semel, sive gradatim & successive impressa fuerit. Et hic motus quoniam in eandem semper plagam cum vi generatrice determinatur, si corpus antea moveatur, motui ejus vel conspiranti additur, vel contrario subducitur, vel obliquo oblique adjicitur, & cum eo secundum utriusque determinationem componitur.

Lex. III.

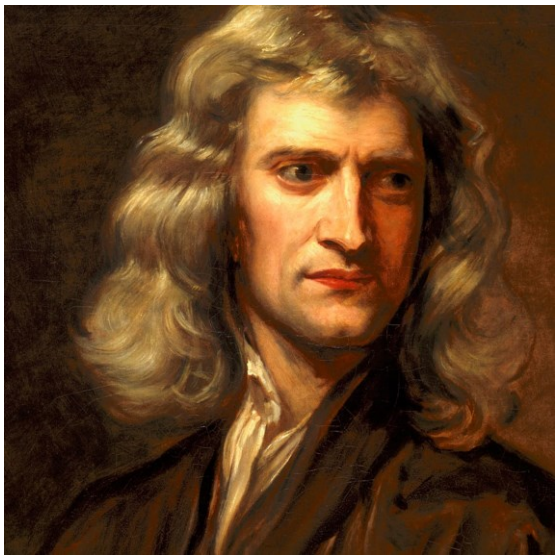
*Actioni contrariam semper & æqualem esse reactionem: sive corporum duorum actiones in se mutuo semper esse æquales & in partes contrarias dirigi.*

Quicquid premit vel trahit alterum, tantundem ab eo premitur vel trahitur. Siquis lapidem digito premit, premitur & hujus digitus a lapide. Si equus lapidem funi allegatum trahit, retrahetur etiam & equus æqualiter in lapidem: nam funis utrinq; distentus eodem relaxandi se conatu urgebit Equum versus lapidem, ac lapidem versus equum, tantumq; impediet progressum unius quantum promovet progressum alterius. Si corpus aliquod in corpus aliud impingens, motum ejus vi sua quomodocunq; mutaverit, ipsum quoque viciſſim in motu proprio eandem mutationem in partem contrariam vi alterius (ob æqualitatem pressionis mutuæ) subibit. His actionibus æquales fiunt mutationes non velocitatum sed motuum, (scilicet in corporibus non aliunde impeditis.) Mutationes enim velocitatum, in contrarias itidem partes factæ, quia motus æqualiter mutantur, sunt corporibus reciproce proportionales.

Corol. I.

*Corpus viribus conjunctis diagonalem parallelogrammi eodem tempore describere, quo latera separatis.*

Si corpus dato tempore, vi sola *M*, ferretur ab *A* ad *B*, & vi sola *N*, ab *A* ad *C*, compleatur parallelogrammum *ABDC*, & vi utraq; ferretur id eodem tempore ab *A* ad *D*. Nam quoniam vis *N* agit secundum lineam *AC* ipsi *BD* parallelam, hæc vis nihil mutabit velocitatem accedendi ad lineam illam *BD* a vi altera genitam. Accedet igitur corpus eodem tempore ad lineam *BD* sive vis *N* imprimatur, sive non, atq; adeo in fine illius temporis reperietur alicubi in linea illa



3

# Gravitational force

- Newton law of gravitation $\mathbf{F}_{12} = G\frac{m_1 m_2}{\mathbf{x}_{12}^3}\mathbf{x}_{12}$
- Individual forces add up linearly

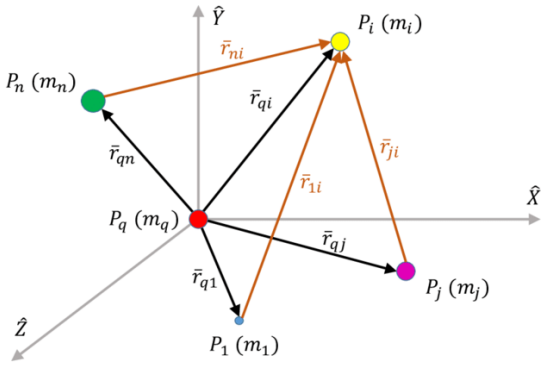
$$\mathbf{F}_1 = Gm_1 \sum_{j\neq 1} \frac{m_j\, \mathbf{x}_{1j}}{\mathbf{x}_{1j}^3}$$

- In the limit of continuous distribution and $m_1 = 1$

$$\mathbf{F}(\mathbf{x}) = G\int \frac{\mathbf{x}' - \mathbf{x}}{|\mathbf{x}' - \mathbf{x}|^3}\rho(\mathbf{x}')d^3\mathbf{x}'$$

- Considering that $\nabla\left(\frac{1}{|\mathbf{x}'-\mathbf{x}|}\right) = \frac{\mathbf{x}'-\mathbf{x}}{|\mathbf{x}'-\mathbf{x}|^3}$
- We can write $\mathbf{F}(\mathbf{x}) = -\nabla\Phi$
- With the gravitational potential

$$\Phi(\mathbf{x}) = -G\int \frac{\rho(\mathbf{x}')}{|\mathbf{x}' - \mathbf{x}|}d^3\mathbf{x}'$$




4

# Poisson equation

- Taking the divergence on both sides of the force equation

$$\boldsymbol{\nabla}\cdot\mathbf{F}(\mathbf{x}) = G\int \nabla_{\mathbf{x}}\cdot\left(\frac{\mathbf{x}'-\mathbf{x}}{|\mathbf{x}'-\mathbf{x}|^3}\right)\rho(\mathbf{x}')d^3\mathbf{x}'$$

- Note that $\nabla\cdot\left(\frac{\mathbf{x}'-\mathbf{x}}{|\mathbf{x}'-\mathbf{x}|^3}\right) = -\frac{3}{|\mathbf{x}'-\mathbf{x}|^3}+\frac{3(\mathbf{x}'-\mathbf{x})\cdot(\mathbf{x}'-\mathbf{x})}{|\mathbf{x}'-\mathbf{x}|^5} = 0 \quad (\mathbf{x}'\neq\mathbf{x})$
- Implies one can restrict integral to small sphere centred on $\mathbf{x}$ and assume $\rho(\mathbf{x})$ constant

$$\boldsymbol{\nabla}\cdot\mathbf{F}(\mathbf{x}) = G\rho(\mathbf{x})\int_{|\mathbf{x}'-\mathbf{x}|\le r}\nabla_{\mathbf{x}}\cdot\left(\frac{\mathbf{x}'-\mathbf{x}}{|\mathbf{x}'-\mathbf{x}|^3}\right)d^3\mathbf{x}' = -G\rho(\mathbf{x})\int_{|\mathbf{x}'-\mathbf{x}|\le r}\nabla_{\mathbf{x}'}\cdot\left(\frac{\mathbf{x}'-\mathbf{x}}{|\mathbf{x}'-\mathbf{x}|^3}\right)d^3\mathbf{x}'$$

- Using the divergence theorem on the surface of the sphere of radius $|\mathbf{x}'-\mathbf{x}| = r$

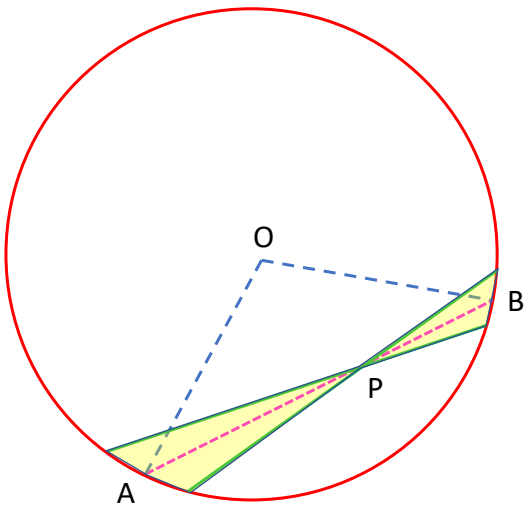
$$\boldsymbol{\nabla}\cdot\mathbf{F}(\mathbf{x}) = -G\rho(\mathbf{x})\int_{|\mathbf{x}'-\mathbf{x}|\le r}\frac{(\mathbf{x}'-\mathbf{x})\cdot d^2\boldsymbol{S}'}{|\mathbf{x}'-\mathbf{x}|^3} = -G\rho(\mathbf{x})\int_{|\mathbf{x}'-\mathbf{x}|\le r}\frac{r\cdot(r^2\,d^2\Omega)}{r^3} = -G\rho(\mathbf{x})\int d^2\,\Omega = -4\pi G\rho(\mathbf{x})$$

- Where $|\mathbf{x}'-\mathbf{x}| = r$ and surface element is $d^2\boldsymbol{S}' = (\mathbf{x}'-\mathbf{x})r\,d^2\Omega$ with $\left|d^2\boldsymbol{S}'\right| = r^2\,d^2\Omega$
- We obtain the Poisson equation relating potential $\Phi$ and density $\rho$: $\nabla^2\Phi(\mathbf{x}) = 4\pi G\rho(\mathbf{x})$

5

# Gravitational force inside spherical shell

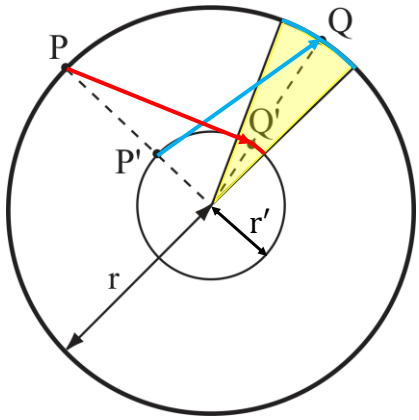
- Consider one thin spherical shell
- Find force on P from shell within two cones
- By symmetry $\widehat{OAP} = \widehat{OBP}$
- Shell surface mass enclosed by cone PA is
- $S_{\mathrm{A}} \propto (\mathrm{PA})^2$
- Force from $S_{\mathrm{A}}$ is $F_A \propto \frac{S_A}{(\mathrm{PA})^2} = k$
- One has $\frac{F_{\mathrm{A}}}{F_{\mathrm{B}}} = 1$
- Zero net force from any two pair of cones
- Newton's 1st theorem
- → No net force inside a spherical shell
- → $\mathbf{F}(\mathbf{x}) = -\boldsymbol{\nabla}\Phi = 0 \Rightarrow \Phi = \mathrm{const}$




6

# Gravitational potential outside spherical shell

- Consider two spherical shells of mass $M$ and radii $\mathrm{r}, \mathrm{r}'$
- Consider the mass enclosed in a given cone
- Contribution to gravitational potential at P due to sector Q′
- $\delta\Phi[\mathbf{x}(\mathrm{P})] = -\frac{\mathrm{GM}}{\mathrm{PQ}'}\frac{\delta\Omega}{4\pi}$
- Contribution to gravitational potential at P′ due to sector Q
- $\delta\Phi'[\mathbf{x}(\mathrm{P}')] = -\frac{\mathrm{GM}}{\mathrm{P}'\mathrm{Q}}\frac{\delta\Omega}{4\pi}$
- But $\mathrm{PQ}' = \mathrm{P}'\mathrm{Q} \Rightarrow \delta\Phi[\mathbf{x}(\mathrm{P})] = \delta\Phi'[\mathbf{x}(\mathrm{P}')]$
- Integrating over the full shells or radii $r$ and $r'$
- $\Phi[\mathbf{x}(\mathrm{P})] = \Phi'[\mathbf{x}(\mathrm{P}')] = \Phi'[\mathbf{x} = 0] = -\frac{GM}{r}$
- Newton's 2nd Theorem
- Potential from the shell is the same as if mass was all concentrated at the origin




7

# Gravitational potential of spherical distributions

- General gravitational potential

$$\Phi(\mathbf{x}) = -G\int \frac{\rho(\mathbf{x}')}{|\mathbf{x}' - \mathbf{x}|}d^3\mathbf{x}'$$

- In spherical symmetry

$$\Phi(r) = -4\pi G\int_0^\infty \rho(r')r'dr' = -G\left[\frac{M(<r)}{r} + 4\pi\int_r^\infty \rho(r')r'dr'\right]$$

$F(r) = -\nabla\Phi(r) = -\frac{GM(<r)}{r^2}$ (no force from outer shells)

- Circular velocity balances gravity and centrifugal forces
- $-F_c(r) = -V_c^2/r = F_G(r) = -\frac{d\Phi}{dr} = -\frac{GM(<r)}{r^2}$
- $V_c^2 = r\frac{d\Phi}{dr} = \frac{GM(<r)}{r}$ good approximation of enclosed mass in real galaxies

8

# Tensor virial equations 1

- Equation of motion for one star attracted by another $\frac{d}{dt}(m_1\mathbf{v}_1) = -\frac{Gm_1m_2}{r^3}\mathbf{r}$
- Equation of motion for one star attracted by a system of N stars

$$\frac{d}{dt}(m_j\mathbf{v}_j) = -\sum_{\substack{k\\k\neq j}} \frac{Gm_jm_k}{|\mathbf{x}_j - \mathbf{x}_k|^3}(\mathbf{x}_j - \mathbf{x}_k)$$

- Consider the $x$ component of $\mathbf{x} \equiv (x, y, z)$, multiply by $y_j$ and sum over all stars

$$\sum_j \frac{d}{dt}(m_j v_{xj}) y_j = -\sum_{\substack{j,k\\k\neq j}} \frac{Gm_jm_k}{|\mathbf{x}_j - \mathbf{x}_k|^3}(x_j - x_k)\, y_j$$

- Write a similar equation for the $k$-th star

$$\sum_k \frac{d}{dt}(m_k v_{xk}) y_k = -\sum_{\substack{j,k\\k\neq j}} \frac{Gm_jm_k}{|\mathbf{x}_j - \mathbf{x}_k|^3}(x_k - x_j)\, y_k$$

9

# Tensor virial equations 2

- Lefthand sides are equal except from a change of index notation

$$\sum_j \frac{d}{dt}(m_j v_{xj}) y_j = \sum_k \frac{d}{dt}(m_k v_{xk}) y_k = \frac{1}{2}\sum_j \frac{d^2}{dt^2}(m_j x_j y_j) - \sum_j m_j v_{xj} v_{yj} = \frac{1}{2}\frac{d^2 I_{xy}}{dt^2} - 2K_{xy}$$

- Where $I_{xy}$ and $K_{xy}$ are components of the inertia and kinetic energy tensors
- Summing the righthand sides gives the $W_{xy}$ component of the potential energy tensor

$$\sum_{\substack{j,k\\k\neq j}} \frac{Gm_jm_k}{|\mathbf{x}_j - \mathbf{x}_k|^3}\left[(x_j - x_k)y_j + (x_k - x_j)y_k\right] = \sum_{\substack{j,k\\k\neq j}} \frac{Gm_jm_k}{|\mathbf{x}_j - \mathbf{x}_k|^3}(x_k - x_j)(y_k - y_j) = 2W_{xy}$$

- Averaging both sides gives one component of the tensor virial equations (Parker 1954)

$$\frac{1}{2}\frac{d^2 I_{xy}}{dt^2} = 2K_{xy} + W_{xy}$$

- In a steady state, and for any pair $ij$ of the $(x, y, z)$ coordinates $2K_{ij} + W_{ij} = 0$

10

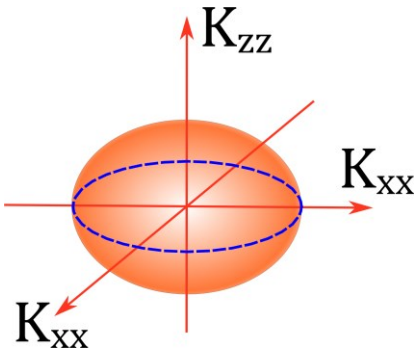
# Scalar virial theorem

- Take the trace $Tr(A) \equiv \sum_i A_{ii}$ of $2K_{ij} + W_{ij} = 0$
- Gives the scalar virial theorem $2K + W = 0$
- Where $K = \frac{1}{2}\sum_j m_j v_j^2$ is the total kinetic energy
- And $W = -\frac{1}{2}\sum_{\substack{j,k \\ k \neq j}} \frac{G m_j m_k}{|\mathbf{x}_j - \mathbf{x}_k|}$ is the total potential energy
- Can be used to measure galaxies/clusters masses

11

# Tensor virial equations in axisymmetry

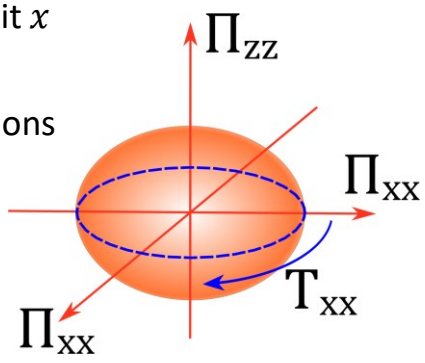
- Assume an oblate galaxy
- Axially symmetric around z-axis
- Tensors must be axially symmetric too
- By symmetry
  - Axial alignment implies non-diagonal elements of $K, W$ tensors must be zero:
  - $K_{xy} = K_{xz} = K_{yz} = 0$ and $W_{xy} = W_{xz} = W_{yz} = 0$
  - Axial symmetry implies $x, y$ components are equal:
  - $K_{xx} = K_{yy}$ and $W_{xx} = W_{yy}$
- The only independent tensor virial equations are
- $2K_{xx} + W_{xx} = 0$ and $2K_{zz} + W_{zz} = 0$
- Like scalar virial equation but for each component separately




12

## Separating rotation in tensor virial equations

- No mean rotation along the $z$ direction, only split $x$
- Start from $2K_{xx} + W_{xx} = 0$
- Split kinetic energy in rotation and random motions
- $K_{xx} \equiv T_{xx} + \Pi_{xx}/2$
- Rotation $T_{xx} + T_{yy} = 2T_{xx} = M\overline{v_\phi^2}/2$
- Random motions $\Pi_{xx} = M\sigma_{xx}^2$
- Mass-weighted average $M\overline{Q} \equiv \sum_k m_k Q_k$
- The tensor virial theorem reduces to
- $2T_{xx} + \Pi_{xx} + W_{xx} = 0$ and $2T_{zz} + \Pi_{zz} + W_{zz} = 0$




13

## Linking rotation and flattening

- Taking the ratio of the two tensor virial equations gives (Binney 1978)

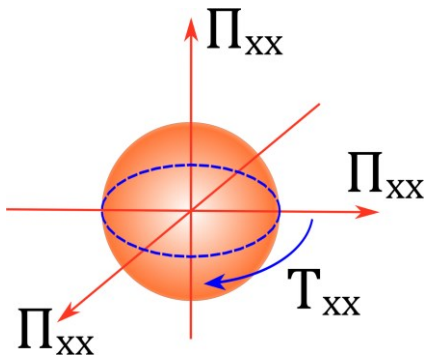
$$\frac{2T_{xx} + \Pi_{xx}}{2T_{zz} + \Pi_{zz}} = \frac{W_{xx}}{W_{zz}}$$

- Usefulness of this equation is that for density distribution that are constant on similar oblate spheroids $\rho(R, z) = \rho(R^2 + z^2/q^2)$ then
- $\frac{W_{xx}}{W_{zz}} = \Omega(q)$
- $\Omega(q) \approx q^{-0.9}$ (4% error for $q = [0.1, 1]$)
- Expression for $\Omega(q)$ e.g. in eq. (15) of Cappellari (2016 ARA&A)

14

# The oblate isotropic rotator benchmark

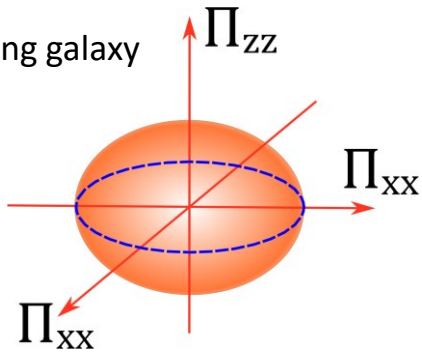
- Assume the velocity dispersion tensor is spherical $\sigma_{ij} = \sigma$
- This assumption has no theoretical justification but it turns out to be a reasonable first order approximation for real galaxies
- $\Pi_{xx} = \Pi_{yy} = \Pi_{zz},\ T_{zz} = 0,\ T_{xx} = T_{yy}$
- With $\Pi_{xx} = M\tilde{\sigma}^2$ and $2T_{xx} = \frac{1}{2}M\tilde{v}^2$
- $\frac{2T_{xx}+\Pi_{xx}}{2T_{zz}+\Pi_{zz}} = \frac{\frac{1}{2}M\tilde{v}^2+M\tilde{\sigma}^2}{M\tilde{\sigma}^2} \approx q^{-0.9}$
- $\left(\frac{\tilde{v}}{\tilde{\sigma}}\right)_{\rm iso} \approx \sqrt{2(q^{-0.9}-1)}$




15

# Anisotropy of a non-rotating galaxy

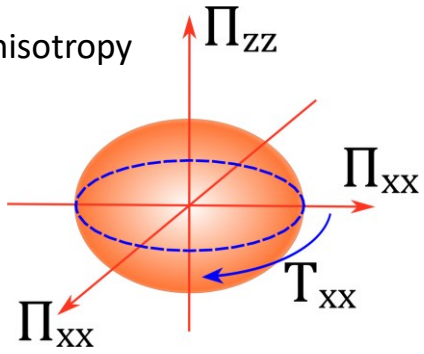
- Consider the limit of an axisymmetric non-rotating galaxy
- $\Pi_{xx} = \Pi_{yy},\ T_{zz} = T_{xx} = T_{yy} = 0$
- $\frac{2T_{xx}+\Pi_{xx}}{2T_{zz}+\Pi_{zz}} = \frac{\Pi_{xx}}{\Pi_{zz}} = \frac{M\tilde{\sigma}_{xx}^2}{M\tilde{\sigma}_{zz}^2} \approx q^{-0.9} \Rightarrow \frac{\tilde{\sigma}_{xx}}{\tilde{\sigma}_{yy}} \approx q^{-0.45}$
- Define global anisotropy parameter
- $\delta = 1 - \frac{\Pi_{zz}}{\Pi_{xx}}$
- E.g. a galaxy with $q = 0.4$ requires
- $\tilde{\sigma}_{xx} \approx 1.5\,\tilde{\sigma}_{yy} \rightarrow \delta \approx 0.56$




16

# $V/\sigma$ of an anisotropic galaxy

- Consider an axisymmetric galaxy with general anisotropy
- $\Pi_{zz} = (1-\delta)\Pi_{xx},\ T_{zz} = 0,\ T_{xx} = T_{yy} = 2T_{xx}$
- $\frac{2T_{xx}+\Pi_{xx}}{2T_{zz}+\Pi_{zz}} = \frac{\frac{1}{2}M\tilde{v}^2+M\tilde{\sigma}^2}{(1-\delta)M\tilde{\sigma}^2} \approx q^{-0.9}$
- $\left(\frac{\tilde{v}}{\tilde{\sigma}}\right)_\delta \approx \sqrt{2[(1-\delta)q^{-0.9}-1]}$
- $\tilde{v}$ and $\tilde{\sigma}$ are mass-weighted intrinsic quantities
- Projection on the sky discussed in Binney (2005)
- Requires integral-field kinematics



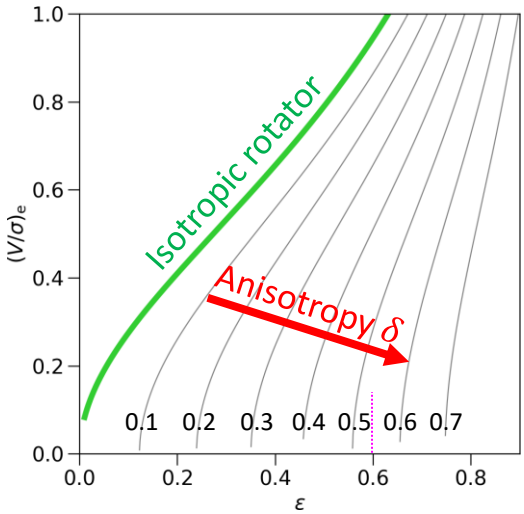

17

# Anisotropy on the $(V/\sigma, \varepsilon)$ diagram

Dominated by rotation

For axisymmetric oblate spheroids

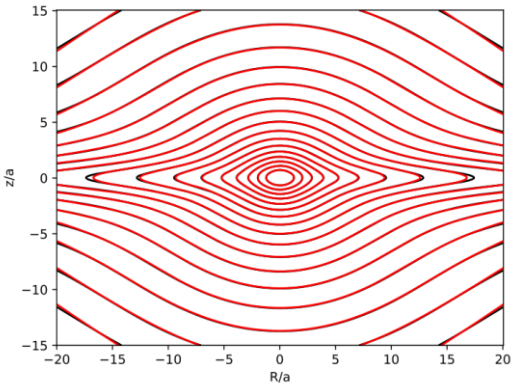
Dominated by random motions




18

# Caveats for the $(V/\sigma, \varepsilon)$ diagram

- Most galaxies are multi-component systems with bulge + disk
- Ellipticity not well defined
- Don't be tempted to study $V/\sigma$ of bulge/disk separately! This is not correct
- At low inclination the difference in ellipticity disappears: many disks classified as elliptical galaxies
- Summations extended to infinite radii but data typically only to half-light radius
- One can use models to estimate the effect of limited data (Cappellari+07)




Realistic galaxy density

19

# Astrophysics C1
# Advanced stellar astrophysics and galaxies
# Lecture 9

**Michele Cappellari**

UNIVERSITY OF OXFORD

1

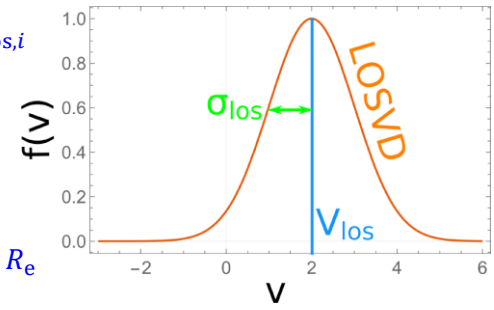
## Grav. potential energy in spherical symmetry

- Defined as the work required to bring all stars to infinity
- $W = -\frac{1}{2}\sum_{\substack{j,k \\ k\neq j}} \frac{Gm_j m_k}{|\mathbf{x}_j - \mathbf{x}_k|} = \frac{1}{2}\sum_j m_j \Phi(\mathbf{x}_j)$
- In the continuum limit $W = \frac{1}{2}\int \rho(\mathbf{x})\Phi(\mathbf{x})dV$
- Assuming spherical symmetry
- $W = -\int_0^\infty \rho(r)\frac{GM(r)}{r} 4\pi r^2 dr = -4\pi G \int_0^\infty \rho(r) M(r)\, r\, dr$
- Example: homogeneous sphere of radius $R$ with $M(r) = \frac{4}{3}\pi\rho r^3$
- $W = -4\pi G \int_0^R r\rho\left(\frac{4}{3}\pi\rho r^3\right) dr = -\frac{16}{15}\pi^2 G\rho^2 R^5 = -\frac{3}{5}\frac{GM^2}{R} \propto -\frac{M^2}{R}$
- The constant is not interesting but proportionality is generally valid

2

# Applying the virial theorem to observations

- For galaxies we don't observe time evolution: assume stead state
- Assume the average motions are isotropic (equal in all directions)
- $K = \frac{1}{2}\sum_i m_i v_i^2 = \frac{1}{2}\sum_i m_i \left(v_x^2 + v_y^2 + v_z^2\right)_i \approx \frac{3}{2}\sum_i m_i v_{\mathrm{los},i}^2$
- For each location $(x', y')$ on the sky plane
- $\sum_i m_i v_{\mathrm{los},i}^2(x', y') = \Sigma(x', y') \int_{-\infty}^{\infty}[\mathrm{f}(v)v^2](x', y')$
- If $\mathrm{f}(v)$ is Gaussian $= \Sigma(x', y')\left(V_{\mathrm{los}}^2 + \sigma_{\mathrm{los}}^2\right)(x', y')$
- Now we need to integrate spatially over the full galaxy
- We measure kinematics e.g. within the half-light radius $R_{\mathrm{e}}$
- $\sigma_{\mathrm{e}}^2 \equiv \overline{V_{\mathrm{rms}}^2} = \sum_j\left[\Sigma\left(x_j, y_j\right)\left(V_{\mathrm{los},j}^2 + \sigma_{\mathrm{los},j}^2\right)\right]$
- $K \propto \sigma_{\mathrm{e}}^2$ and from previous slide $W \propto -\frac{M^2}{R}$
- Virial theorem $K = -\frac{W}{2}$ implies $\sigma_{\mathrm{e}}^2 \propto \frac{M^2}{R} \Rightarrow M \propto R\sigma_{\mathrm{e}}^2$




3

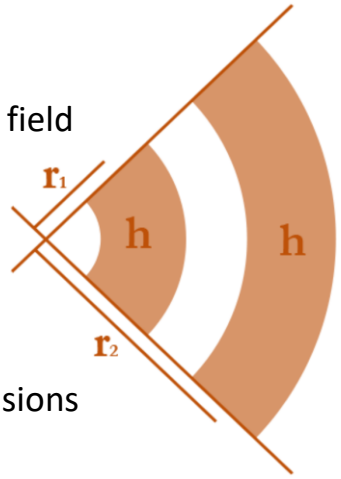
# Measuring virial mass-to-light ratios

- Galaxy mass is empirically generally a poorly-defined quantity
  - Kinematic data generally extend to a limited extent
  - Outer profile not well defined
- Instead of masses one can accurately measure mass-to-light
- The virial theorem suggests $M \propto R\sigma^2 \Rightarrow (M/L)_{\mathrm{vir}} = k\frac{R\sigma^2}{LG}$
- The constant could be determined using simple analytic models
- But better determined using calibration with dynamical models
- When galaxy size is the half-light radius $R_e$ one finds $k \approx 5.0$
- $(M/L)_{\mathrm{vir}} = 5.0\frac{R_e\sigma_e^2}{LG}$ (Cappellari+06)
- But details of how to measure parameters are important

4

# Gravity is long-range force

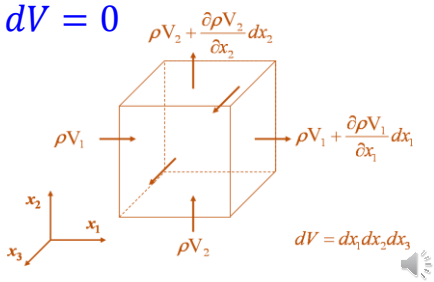
- The key difference between motions of stars and molecules is the nature of the gravitational force
- Consider a cone from a location within the density field of a galaxy
- $m_1 \propto r_1^2 h$ and $m_2 \propto r_2^2 h$
- $f_1 \propto \frac{Gm_2}{r_1^2} \propto h$ and $f_2 \propto \frac{Gm_2}{r_2^2} \propto h$
- Implies that distant stars dominate the net force
- Unlike molecules where force only acts during collisions




5

# General continuity equation

- Consider a volume $V$ bounded by a surface $S$ enclosing a mass $M(t)$
- Mass flowing through $S$ is equal to the change of $M(t)$ in $V$
- $\int_S \rho \mathbf{v} \cdot d\mathbf{S} = -\frac{dM}{dt} = -\frac{\partial}{\partial t}\int_V \rho \, dV = -\int_V \frac{\partial \rho}{\partial t} dV$
- Using the divergence theorem $\int_S \mathbf{Q} \cdot d\mathbf{S} = \int_V \nabla \cdot \mathbf{Q} \, dV$
- $\int_V \frac{\partial \rho}{\partial t} dV + \int_V \nabla \cdot (\rho \mathbf{v}) \, dV = \int_V \left[\frac{\partial \rho}{\partial t} + \nabla \cdot (\rho \mathbf{v})\right] dV = 0$
- Given that the volume is generic
- One obtains the continuity equation
- $\frac{\partial \rho}{\partial t} + \nabla \cdot (\rho \mathbf{v}) = 0$



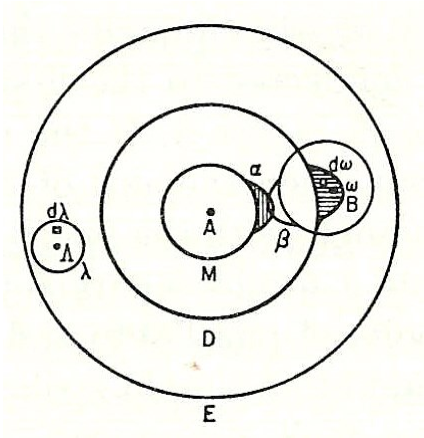

6

# The distribution function (DF)

- The DF or phase-space density $f(\mathbf{x}, \mathbf{v}, t) d^3\mathbf{x}\, d^3\mathbf{v}$ gives a full description of any collisionless system
- It specifies the number of stars with positions in the small volume $d^3\mathbf{x}$ and velocities in the ranges $d^3\mathbf{v}$
- When normalized, DF is the probability for a start to be in $d^3\mathbf{x}\, d^3\mathbf{v}$
- Define the 6-dim phase-space vector $\mathbf{w} = (\mathbf{x}, \mathbf{v}) = (\mathbf{w_1}, \mathbf{w_2}, \ldots, \mathbf{w_6})$
- The flow in phase-space is $\dot{\mathbf{w}} = (\dot{\mathbf{x}}, \dot{\mathbf{v}}) = (\mathbf{v}, -\boldsymbol{\nabla}\Phi)$
- $\dot{\mathbf{w}}$ is related to $\mathbf{w}$ like the fluid velocity to the coordinates in a 3D fluid

7

# Ludwig Boltzmann 1844-1906






8

# The Collisionless Boltzmann Equation (CBE) 1

- The continuity equation for a 6D fluid of stars in phase-space is called the Collisionless Boltzmann Equation
- $\frac{\partial f}{\partial t} + \nabla \cdot (f \dot{\mathbf{w}}) = 0$
- This can be expanded out as
- $\frac{\partial f}{\partial t} + \sum_k^6 \left( \dot{w}_k \frac{\partial f}{\partial w_k} + f \frac{\partial \dot{w}_k}{\partial w_k} \right) = 0$
- Separating positions and velocities derivatives in the last term
- $\frac{\partial f}{\partial t} + \sum_k^6 \dot{w}_k \frac{\partial f}{\partial w_k} + f \sum_i^3 \left[ \frac{\partial v_i}{\partial x_i} + \frac{\partial \dot{v}_i}{\partial v_i} \right] = 0$

9

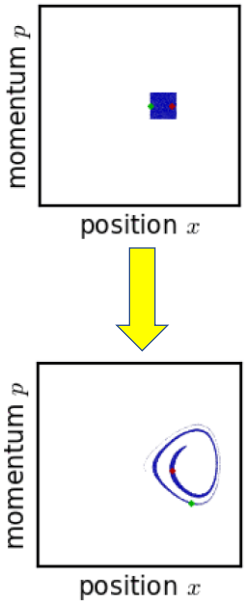
# The Collisionless Boltzmann Equation (CBE) 2

- As $x$ and $v$ are independent phase-space coordinates $\frac{\partial v_i}{\partial x_i} = 0$
- Also $\frac{\partial \dot{v}_i}{\partial v_i} = \frac{\partial}{\partial v_i} \left( -\frac{\partial \Phi}{\partial x_i} \right) = 0$ as $\nabla\Phi$ is independent of velocities
- This leaves $\frac{\partial f}{\partial t} + \sum_k^6 \dot{w}_k \frac{\partial f}{\partial w_k} = 0$
- Separating again positions and velocities derivatives
- $\frac{\partial f}{\partial t} + \sum_i^3 \left( v_i \frac{\partial f}{\partial x_i} + \dot{v}_i \frac{\partial f}{\partial v_i} \right) = 0$ and replacing $\dot{v}_i = -\frac{\partial \Phi}{\partial x_i}$
- $\frac{\partial f}{\partial t} + \sum_i^3 \left( v_i \frac{\partial f}{\partial x_i} - \frac{\partial \Phi}{\partial x_i} \frac{\partial f}{\partial v_i} \right) = 0$ or in vector notation
- $\frac{\partial f}{\partial t} + (\mathbf{v} \cdot \nabla f) - \left( \nabla\Phi \cdot \frac{\partial f}{\partial \mathbf{v}} \right)$ is the collisionless Boltzmann equation

10

# CBE = Liouville theorem

- Given that $f = f(\mathbf{x}, \mathbf{v}, t)$
- Take the Lagrangian derivative for an observer moving with $\mathbf{v}$
- $df = \frac{\partial f}{\partial t} dt + \sum_i^3 \left( \frac{\partial f}{\partial x_i} dx_i + \frac{\partial f}{\partial v_i} dv_i \right)$
- $\frac{df}{dt} = \frac{\partial f}{\partial t} + \sum_i^3 \left( \frac{\partial f}{\partial x_i} v_i + \frac{\partial f}{\partial v_i} \dot{v}_i \right) = \frac{\partial f}{\partial t} + \sum_i^3 \left( v_i \frac{\partial f}{\partial x_i} - \frac{\partial \Phi}{\partial x_i} \frac{\partial f}{\partial v_i} \right) = \text{CBE}$
- The CBE then simply states that $\frac{df}{dt} = 0$
- The Lagrangian derivative along trajectories in phase space is zero
- The phase-space density around a star in phase-space is constant
- The phase-space flow is incompressible




11

# James Jeans 1877-1946

*The Motions of the Stars in a Kapteyn-Universe.*
By J. H. Jeans.

1. In his recent paper "On the Distribution of the Stars in Space,"* and again in his "First Attempt at a Theory of the Arrangement and Motion of the Sidereal System,"† Professor Kapteyn has given a masterly summary of our present knowledge, mainly due to his own researches, of the arrangement of the stars in space. In brief, he finds that the arrangement of the stars may be regarded, with very tolerable accuracy, as consisting of a system of spheroidal shells, each of constant density. The spheroids are similar and similarly situated; they are oblate, having their axes in the ratio 5·102 : 5·102 : 1, their equal longer axes being in the galactic plane and their common centre being not far removed from the position of the sun.

In the second of these papers Professor Kapteyn attempts a dynamical investigation of such a system of stars. He assumes that the stars are in a dynamically steady state, and makes the further supposition that along the shortest axes of these spheroids (*i.e.* in the directions of the galactic poles) the law of distribution is Maxwell's well-known law for the distribution of molecular velocities of a gas in isothermal equilibrium.

Kapteyn's first assumption can neither be proved nor disproved; in the present state of our knowledge it is probably the most reasonable assumption to take as the basis of a dynamical discussion. But, for

* *Astrophys. Journ.*, 52 (1920), 23. † *Ibid.* (1922).

reasons which will appear later, the second assumption seems much less plausible. Indeed, in introducing it Kapteyn writes: "We will now introduce some considerations from the kinetic theory of gases, the applicability of which to the stellar system might be considered doubtful. . . . The results which will be derived cannot lay claim to be demonstrably correct."

The main object of the present paper is to show that the introduction of Kapteyn's dubious second assumption is unnecessary. As we shall now see, the principal features of the motion of the stars can be deduced from a knowledge of their distribution in space, combined only with the single assumption that the system of stars is in a steady state.



12

# Jeans equations 1

- CBE is rather useless as it stand
- One differential equation to define a function $f(t, \mathbf{x}, \mathbf{v})$ of 7 variables!
- The Jeans equation reduce CBE to equations for velocity moments
- We consider a tracer population of stars with DF $f$ in steady-state orbiting in a fixed gravitational potential $\Phi$
- NB: The tracer does not have to follow the light of the galaxy
- The tracer could be a subset like e.g. the planetary nebulae in a galaxy
- It could be e.g. the globular clusters assumed point-like particles
- Define the mean $\overline{Q(\mathbf{x})} = \frac{\int Q(\mathbf{x}) f(\mathbf{x},\mathbf{v})\, d^3\mathbf{v}}{\int f(\mathbf{x},\mathbf{v})\, d^3\mathbf{v}} = \frac{1}{\rho}\int Q(\mathbf{x}) f(\mathbf{x},\mathbf{v})\, d^3\mathbf{v}$
- Where the density of the tracer is $\rho(\mathbf{x}) = \int f(\mathbf{x},\mathbf{v})\, d^3\mathbf{v}$

13

# Jeans equations 2

- Start from CBE assuming steady state $\sum_i^3 \left( v_i \frac{\partial f}{\partial x_i} - \frac{\partial \Phi}{\partial x_i}\frac{\partial f}{\partial v_i} \right) = 0$
- Multiply the CBE by a generic function $Q(\mathbf{x})$ and integrate over $\mathbf{v}$

$$\sum_i^3 \int Q v_i \frac{\partial f}{\partial x_i} d^3\mathbf{v} - \sum_i^3 \int Q \frac{\partial \Phi}{\partial x_i}\frac{\partial f}{\partial v_i} d^3\mathbf{v} = 0$$

- Take the time and space derivatives outside the velocity integrals

$$\sum_i^3 \frac{\partial}{\partial x_i} \int Q v_i f\, d^3\mathbf{v} - \sum_i^3 \frac{\partial \Phi}{\partial x_i} \int Q \frac{\partial f}{\partial v_i} d^3\mathbf{v} = 0$$

$$\sum_i^3 \frac{\partial (\rho \overline{Q v_i})}{\partial x_i} - \sum_i^3 \frac{\partial \Phi}{\partial x_i} \int Q \frac{\partial f}{\partial v_i} d^3\mathbf{v} = 0$$

14

## Jeans equations 3

- Take the second term of the last equation
- Using integration by parts
- $\int Q \frac{\partial f}{\partial v_i} d^3\mathbf{v} = \iint [Qf]_{v_i=-\infty}^{v_i=+\infty} dv_j dv_k - \int \frac{\partial Q}{\partial v_i} f d^3\mathbf{v}$
- One has $[Qf]_{v_i=-\infty}^{v_i=+\infty} = 0$ assuming $Qf = 0$ for $|\mathbf{v}| \to \infty$
- And by definition $\int \frac{\partial Q}{\partial v_i} f d^3\mathbf{v} = \rho \overline{\frac{\partial Q}{\partial v_i}}$
- The last equation on the previous slides becomes
- $\sum_i^3 \frac{\partial (\rho \overline{Q v_i})}{\partial x_i} + \rho \sum_i^3 \frac{\partial \Phi}{\partial x_i} \overline{\frac{\partial Q}{\partial v_i}} = 0$

15

## Jeans equations 4

- Last equation is valid for a generic function $Q(\mathbf{x})$
- $\sum_i^3 \frac{\partial (\rho \overline{Q v_i})}{\partial x_i} + \rho \sum_i^3 \frac{\partial \Phi}{\partial x_i} \overline{\frac{\partial Q}{\partial v_i}} = 0$
- With $Q = 1$ on has $\partial Q / \partial v_i = 0$
- Top equation becomes steady-state continuity equation
- $\sum_i^3 \frac{\partial (\rho \overline{v_i})}{\partial x_i} = 0$
- With $Q = v_j$ one has $\overline{\partial v_j / \partial v_i} = \delta_{ij}$
- The top equation gives three force equations for $j = 1, 2, 3$
- $\sum_i^3 \frac{\partial (\rho \overline{v_i v_j})}{\partial x_i} + \rho \frac{\partial \Phi}{\partial x_j} = 0$

16

# Jeans equations 5

- Force equations generally rewritten separating random and ordered motions
- Multiply the continuity equation by $\overline{v_j}$
- $\overline{v_j}\sum_i^3 \frac{\partial(\rho\overline{v_i})}{\partial x_i} = \sum_i^3 \frac{\partial(\rho\overline{v_i}\,\overline{v_j})}{\partial x_i} - \rho\sum_i^3 \overline{v_i}\frac{\partial \overline{v_j}}{\partial x_i} = 0$
- Subtract this from the moments equations
- $\sum_i^3 \frac{\partial(\rho\overline{v_i v_j})}{\partial x_i} + \rho\frac{\partial\Phi}{\partial x_j} - \sum_i^3 \frac{\partial(\rho\overline{v_i}\,\overline{v_j})}{\partial x_i} + \rho\sum_i^3 \overline{v_i}\frac{\partial \overline{v_j}}{\partial x_i} = 0$
- Use the definition of velocity dispersion tensor $\sigma_{ij}^2 = \overline{v_i v_j} - \overline{v_i}\,\overline{v_j}$
- Finally gives the three Jeans equations for $j = 1, 2, 3$

$$\sum_i^3 \frac{\partial(\rho\sigma_{ij}^2)}{\partial x_i} + \rho\sum_i^3 \overline{v_i}\frac{\partial \overline{v_j}}{\partial x_i} = -\rho\frac{\partial\Phi}{\partial x_j}$$

17

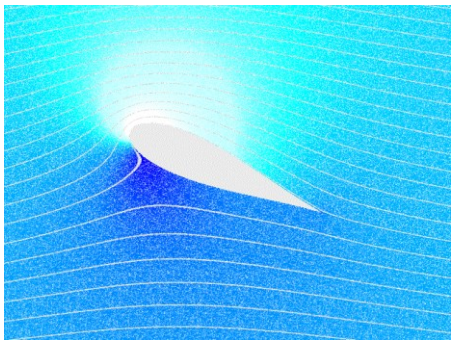
# Jeans equations as stellar hydrodynamics

- In vector form the Jeans equations can be written
- $\rho(\overline{\mathbf{v}}\cdot\nabla)\overline{\mathbf{v}} + \nabla(\rho\boldsymbol{\sigma}^2) = -\rho\nabla\Phi$
- A similar equation can be derived in fluid dynamics for a fluid element
- Equation of motion $\rho\frac{d\mathbf{v}}{dt} = -\boldsymbol{\nabla}P - \rho\boldsymbol{\nabla}\Phi_{\text{ext}}$
- Where $\mathbf{v} = \mathbf{v}(\mathbf{x}, t)$ and $d\mathbf{v} = \frac{\partial\mathbf{v}}{\partial t}dt + \sum_i^3 \frac{\partial\mathbf{v}}{\partial x_i}dx_i$ then $\frac{d\mathbf{v}}{dt} = \frac{\partial\mathbf{v}}{\partial t} + (\mathbf{v}\cdot\boldsymbol{\nabla})\mathbf{v}$
- Equation of motion, in steady-state $\partial\mathbf{v}/\partial t = 0$, become the Euler equations
- $\rho(\mathbf{v}\cdot\nabla)\mathbf{v} + \boldsymbol{\nabla}P = -\rho\boldsymbol{\nabla}\Phi_{\text{ext}}$
- The role of pressure is represented by velocity dispersion $P \to \rho\sigma_{ij}^2$
- But instead of scalar pressure we have a stress tensor
- However, no equation of state relating $\sigma_{ij}^2 \to \rho$, unlike gas $P \to f(\rho, T)$

18

# Non uniqueness of the Jeans equations

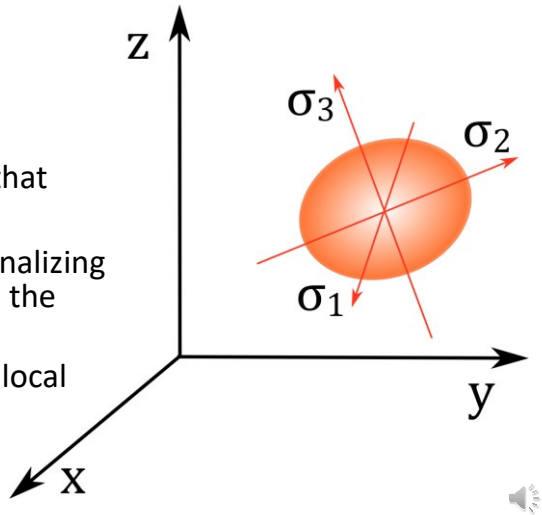
- The 3 Jeans equations have 9 unknown
- 6 for the symmetric $\sigma_{ij}^2$ tensor
- $\sigma_{ij}^2 \equiv \begin{pmatrix} \sigma_{xx}^2 & \sigma_{xy}^2 & \sigma_{xz}^2 \\ \sigma_{yx}^2 & \sigma_{yy}^2 & \sigma_{yz}^2 \\ \sigma_{zx}^2 & \sigma_{zy}^2 & \sigma_{zz}^2 \end{pmatrix}$ with $\sigma_{ij}^2 = \sigma_{ji}^2$
- 3 for streaming motions $\overline{v_j}$
- The 3 Euler equations for fluid have 4 unknown
- 1 scalar pressure $P$
- 3 for streaming motions $v_j$
- For fluids the equation of state $P \rightarrow f(\rho, T)$ "closes" the equations



19

# The velocity ellipsoid

- $\sigma_{ij}^2 \equiv \begin{pmatrix} \sigma_{xx}^2 & \sigma_{xy}^2 & \sigma_{xz}^2 \\ \sigma_{yx}^2 & \sigma_{yy}^2 & \sigma_{yz}^2 \\ \sigma_{zx}^2 & \sigma_{zy}^2 & \sigma_{zz}^2 \end{pmatrix}$ with $\sigma_{ij}^2 = \sigma_{ji}^2$
- One may chose a local coordinate system that diagonalizes $\sigma_{ij}^2 = \mathrm{diag}(\sigma_1^2, \sigma_2^2, \sigma_3^2)$
- The ellipsoid aligned with the locally diagonalizing coordinates, with axes $(\sigma_1, \sigma_2, \sigma_3)$ is called the Velocity Ellipsoid
- Its length along a given direction gives the local velocity dispersion $\sigma$ along that direction




20

# Astrophysics C1
# Advanced stellar astrophysics and galaxies
# Lecture 10

**Michele Cappellari**

UNIVERSITY OF OXFORD

1

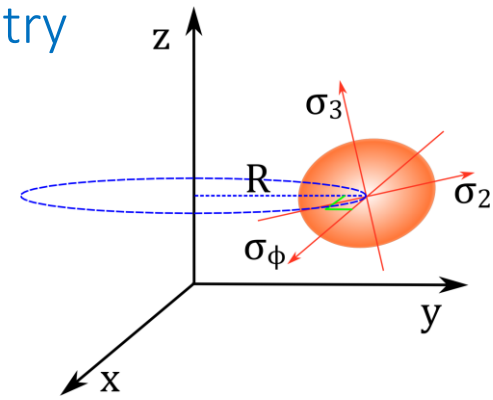
## CBE in cylindrical coordinates

- Jeans equations almost never used in Cartesian coordinates
- Spherical or cylindrical coordinates allow us to enforce symmetries
- To derive in a different coordinate system is easier to start from CBE
- Valid in any coordinate systems $\sum_i^3 \left( v_i \frac{\partial f}{\partial x_i} - \frac{\partial \Phi}{\partial x_i} \frac{\partial f}{\partial v_i} \right) = 0$
- In cylindrical coordinate system $(R, \phi, z)$ becomes
- $\dot{R} \frac{\partial f}{\partial R} + \dot{\phi} \frac{\partial f}{\partial \phi} + \dot{z} \frac{\partial f}{\partial z} + \dot{v}_R \frac{\partial f}{\partial v_R} + \dot{v}_\phi \frac{\partial f}{\partial v_\phi} + \dot{v}_z \frac{\partial f}{\partial v_z} = 0$
- After some transformations (e.g. Sec. 4.1(a) of Binney & Tremaine 1987)
- $v_R \frac{\partial f}{\partial R} + v_z \frac{\partial f}{\partial z} + \left( \frac{v_\phi^2}{R} - \frac{\partial \Phi}{\partial R} \right) \frac{\partial f}{\partial v_R} - \frac{\partial \Phi}{\partial z} \frac{\partial f}{\partial v_z} - \frac{v_R v_\phi}{R} \frac{\partial f}{\partial v_\phi} = 0$

2

# Jeans equations in axisymmetry

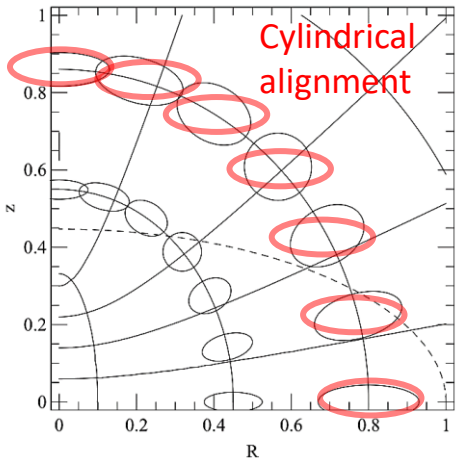
- Assume the galaxy is axisymmetric and in steady state
- By symmetry
  - $\overline{v_R} = \overline{v_z} = 0$ and $\overline{v_R v_\phi} = \overline{v_z v_\phi} = 0$
  - $\partial\Phi/\partial\phi = \partial f/\partial\phi = 0$
  - But $\overline{v_R v_z} \neq 0$
- Same procedure as the Cartesian case
- Multiply by $v_R$ and then $v_z$, and integrate over velocity
- $\frac{\rho\overline{v_R^2} - \rho\overline{v_\phi^2}}{R} + \frac{\partial\left(\rho\overline{v_R^2}\right)}{\partial R} + \frac{\partial(\rho\overline{v_R v_z})}{\partial z} = -\frac{\rho\partial\Phi}{\partial R}$
- $\frac{\rho\overline{v_R v_z}}{R} + \frac{\partial\left(\rho\overline{v_z^2}\right)}{\partial z} + \frac{\partial(\rho\overline{v_R v_z})}{\partial R} = -\frac{\rho\partial\Phi}{\partial z}$
- Two equations and four unknown: $\overline{v_R^2}$, $\overline{v_z^2}$, $\overline{v_\phi^2}$ and $\overline{v_R v_z}$ → No unique solution




3

# Observed shape of velocity ellipsoid

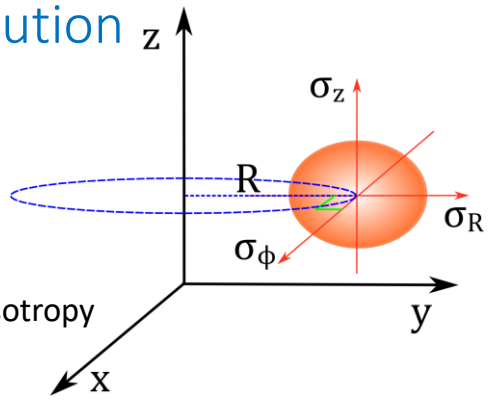
- Velocity ellipsoid from general models
- Nearly spherically aligned beyond 1Re
- $\sigma_R \approx \sigma_\phi$
- $\sigma_z < \sigma_R$ on equatorial plane & symmetry axis (Cappellari+07; Thomas+09)
- Cylindrical alignment agrees on equatorial plane and symmetry axis
- Best first-order approximation with constant anisotropy




(Cappellari 2008)

4

# Cylindrically aligned Jeans solution

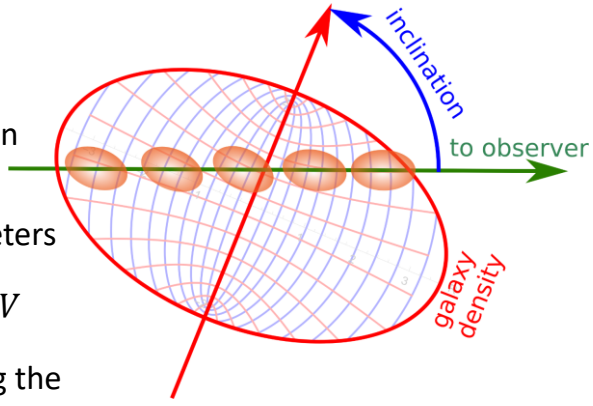



- Start from general axisymmetric equations
- $\frac{\rho\overline{v_R^2}-\rho\overline{v_\phi^2}}{R}+\frac{\partial\left(\rho\overline{v_R^2}\right)}{\partial R}+\frac{\partial(\rho\overline{v_R v_z})}{\partial z}=-\frac{\rho\partial\Phi}{\partial R}$
- $\frac{\rho\overline{v_R v_z}}{R}+\frac{\partial\left(\rho\overline{v_z^2}\right)}{\partial z}+\frac{\partial(\rho\overline{v_R v_z})}{\partial R}=-\frac{\rho\partial\Phi}{\partial z}$
- Assume cylindrical alignment and constant anisotropy
- → $\overline{v_R v_z}=0$ and $\overline{v_R^2}=b\overline{v_z^2}$ or $\sigma_R^2=b\sigma_z^2$
- $\frac{b\rho\sigma_z^2-\rho\overline{v_\phi^2}}{R}+\frac{\partial\left(b\rho\sigma_z^2\right)}{\partial R}=-\rho\frac{\partial\Phi}{\partial R}$
- $\frac{\partial\left(\rho\sigma_z^2\right)}{\partial z}=-\rho\frac{\partial\Phi}{\partial z}$
- 2 eq. and 2 var. → Unique solution but does it approximate real galaxies?

5

# Apply Jeans equations to real galaxies

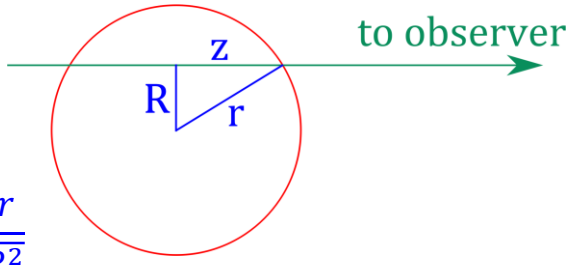
- One need the tracer distribution $\rho$
- Can be inferred from the galaxy surface brightness (NB: not stellar mass)
- Need to assume a total mass distribution luminous + dark + gas
- This is what we want to measure: use parametrization with some free parameters (e.g. dark matter fraction and $M_*/L$)
- We observe mean line-of-sight velocity $V$ and velocity dispersion $\sigma$
- Need to project velocity moments along the line-of-sight (except for Milky Way)
- $\Sigma\overline{v_{\rm los}^2}(x,y)=\int_{-\infty}^{\infty}\rho\overline{v_{\rm los}^2}(x,y,z)dz$




Line-of-sight integration of the velocity ellipsoid

6

# From intrinsic to projected density




- Assume spherical symmetry
- Luminosity distribution $\rho(r)$
- Projected surface brightness $\Sigma(R)$

$$\Sigma(R) = 2\int_0^\infty \rho(r)dz = 2\int_R^\infty \frac{\rho(r)rdr}{\sqrt{r^2+R^2}}$$

- This is an Abel integral with inverse
- $\rho(r) = -\frac{1}{\pi}\int_r^\infty \frac{d\Sigma}{dR}\frac{dR}{\sqrt{R^2-r^2}}$
- Requires a derivative $d\Sigma/dR$ which is noisy on real data
- More robust to assume a form of $\rho(r)$ and fit to the $\Sigma(R)$ data

7

# Schwarzschild's (1979) method

- Assume steady state
- Distribution function DF only function of isolating integral of motions (Jeans's theorem)
- In other words: orbital distribution depends on orbits
- $\mathrm{DF} = f(x, y, z, v_x, v_y, v_z) = f(\boldsymbol{I})$
- Find complete set of basis functions for DF
- Key idea of Schwarzschild: basis functions $F_j$ are stellar orbits
- $\mathrm{DF} = \sum_j w_j F_j(\boldsymbol{I})$
- Observables (e.g., kinematics) are linear function of orbits
- → observables are linear superposition of orbital observables
- $O_\alpha(x', y') = \sum_j G_\alpha[F_j(\boldsymbol{I})]$

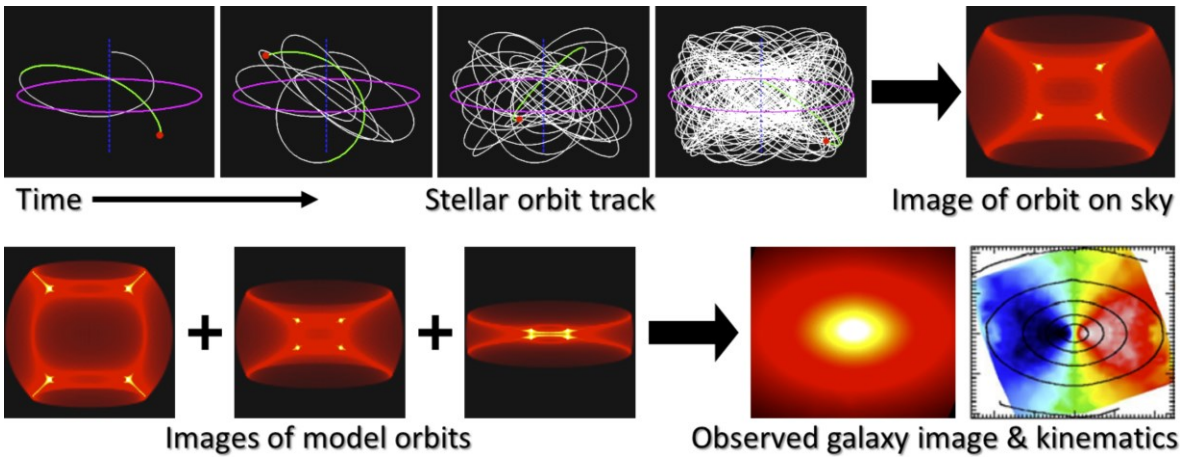
8

## Fit orbits to observables

- With *N* orbits and *M* observables to fit
- Problem to solve in the least-squares sense:
- $$\begin{pmatrix} p_{1,1} & \cdots & p_{1,N} \\ \vdots & \ddots & \vdots \\ p_{M,1} & \cdots & p_{M,N} \end{pmatrix} \begin{pmatrix} w_1 \\ \vdots \\ w_N \end{pmatrix} = \begin{pmatrix} o_1 \\ \vdots \\ o_M \end{pmatrix}$$
- $\min_x \{\|\boldsymbol{A}x - b\|\}$ with $x > 0$
- Is a Non-Negative Least-Squares (NNLS) problem
- Has a unique (possibly degenerate) minimum
- Efficient algorithms exist (NNLS or quadratic programming)

9

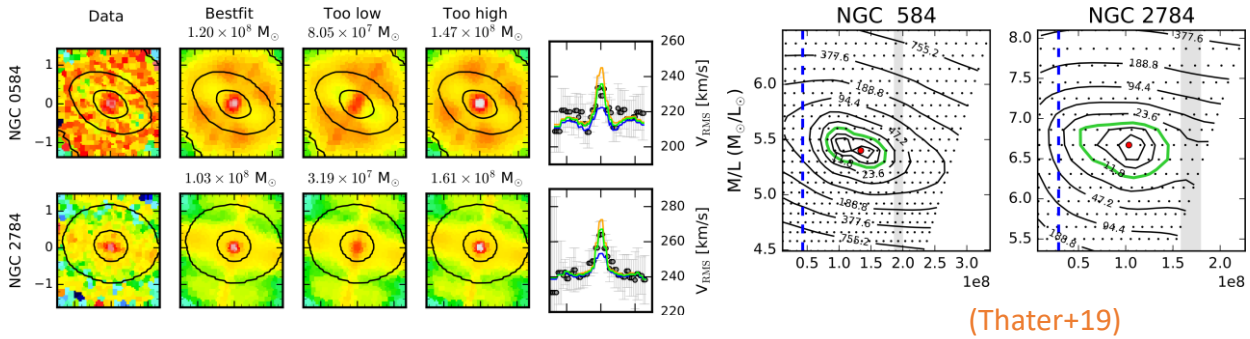
## Orbital-superposition method




Cappellari (2015 IAUS)

10

# Example: measuring supermassive black holes




(Thater+19)

- Vary two key parameters (i) black hole mass and (ii) galaxy M/L
- For every set of parameter re-compute the orbit library and re-fit to the data
- Find the set of orbits that better fits the data (e.g., minimum $\chi^2$)

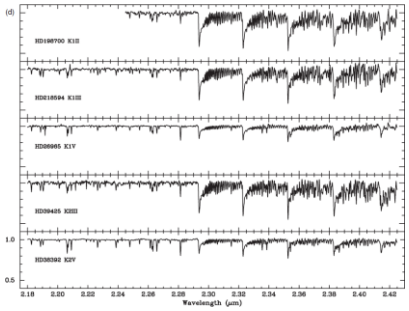
11

# Galaxies stellar kinematics

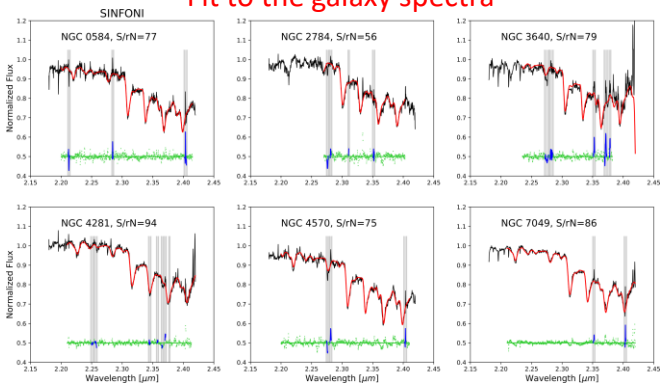
12

# Extracting stellar absorption-line kinematics

Stellar templates



Fit to the galaxy spectra



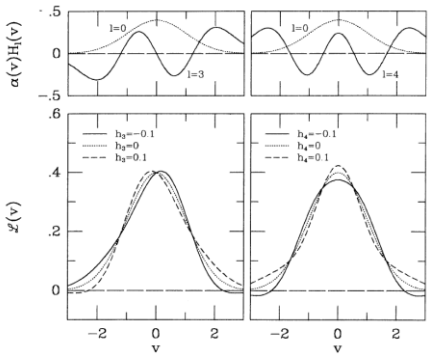

- $G(\lambda) = S(\lambda) \otimes L(V_{los})$
- Good stellar template essential
- Allow for calibration inaccuracies
- $G(\lambda) = \sum_j [w_j S_j(\lambda) \otimes L(V_{los})] + \sum_l b_l P_l(\lambda)$

(Thater+19)

13

# Parametrizing the line-of-sight velocity distribution

- Line-of-sight velocity distribution $L(V)$
- To first order well approximated by a Gaussian
- → $L(V)$ Commonly described by deformed Gaussian
- $L(V) = \exp\left[-\frac{(V-V_0)^2}{2\sigma^2}\right][1 + h_3 H_3(V) + h_4 H_4(V)]$
- $H_j$ are Hermite polynomials: orthogonal expansion




Van der Marel & Franx (1993)

14

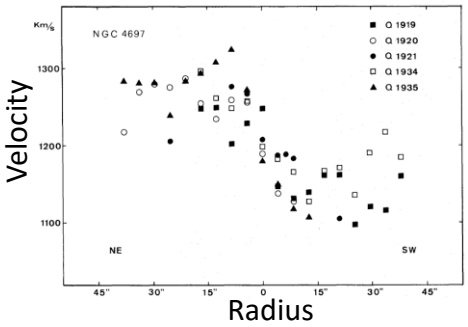
# First rotation curve of an elliptical galaxy

DYNAMICS OF EARLY TYPE GALAXIES. I. THE ROTATION CURVE OF THE ELLIPTICAL GALAXY NGC 4697

F. BERTOLA AND M. CAPACCIOLI
Asiago Astrophysical Observatory, University of Padova; Institute of Physics, University of Lecce
*Received 1974 September 9; revised 1975 February 14*

ABSTRACT

The rotation curve, up to 0.6 from the center, has been derived from Ca II H and K lines for the elliptical galaxy NGC 4697. A maximum seems to be reached at 15″ with 65 km s$^{-1}$. The same galaxy has been investigated by means of photographic photometry in the *B* system. The luminosity profile follows the $r^{1/4}$ law, and the mean ellipticity is 0.4. The total apparent magnitude is $B = 10.30$ mag, and the corresponding absolute magnitude reaches $M_B = -20.5$ mag, assuming a distance of 14.8 Mpc. The spatial velocity curve and the light density profile are derived. Mass and angular momentum have been computed on the hypothesis that the mass-to-light ratio is constant through the galaxy, leaving it as a free parameter. Under several assumptions it is found that the angular momentum of the elliptical NGC 4697 is lower than that of a spiral of comparable mass by a factor 5 to a factor 30, when the mass-to-light ratio varies from 5 to 50.

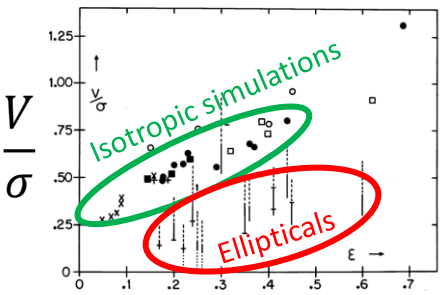



(Bertola+Capaccioli75)

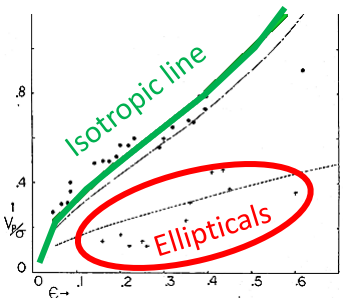
- Elliptical galaxy NGC4697
- 2 hr of observations at 5-m Palomar
- Angular momentum much lower than spirals

15

# Introducing the $(V/\sigma, \varepsilon)$ diagram




(Illingworth77)

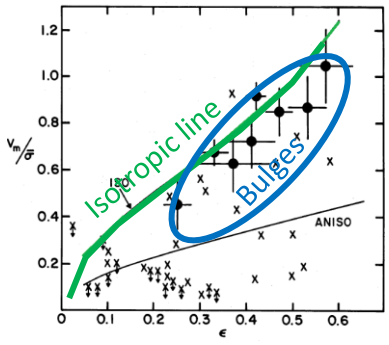



(Binney78)

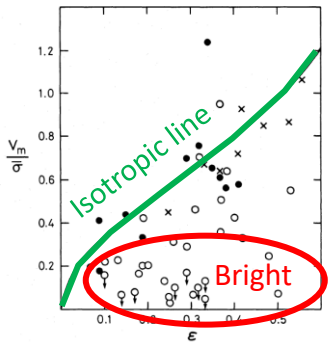
- Sample of 13 ellipticals (Illingworth77)
- Less rotation than isotropic simulations
- Isotropic line from tensor virial theorem (Binney78)

16

# Kinematics depends on luminosity




(Kormendy+Illingworth82; K82)

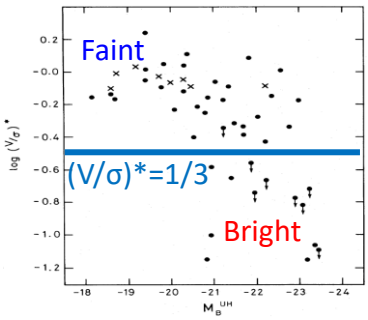



(Davies+83)

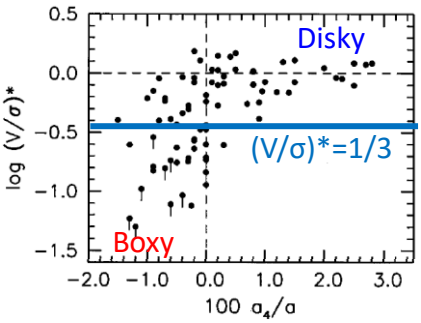
- Bulges close to isotropic (Kormendy+Illingworth82)
- Bulges like faint ellipticals (Davies+83)
- But bright ellipticals rotate slowly

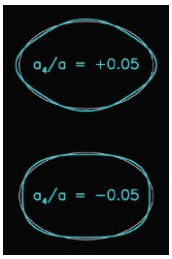
17

# $(V/\sigma)^*$ follows galaxy luminosity




(Davies+83)



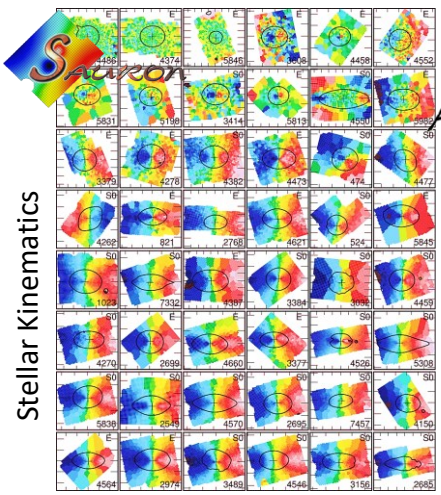



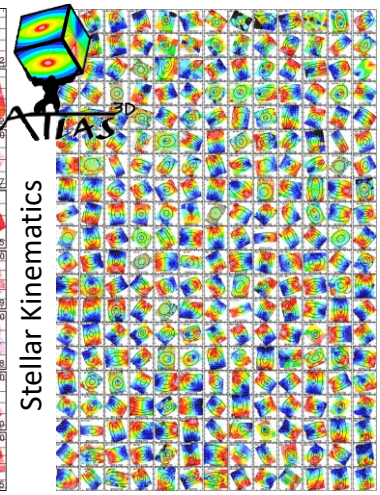

(Bender88; Kormendy+Bender96)

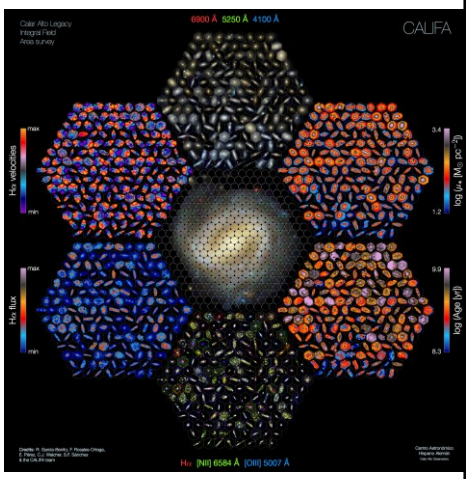
- $(V/\sigma)^* \equiv (V/\sigma) \,/\, (V/\sigma)_{ISO}$ (Kormendy+Illingworth82; Davies+83)
- Faint ellipticals only for $(V/\sigma)^* > 1/3$ (Davies+83)
- Similarly, disky galaxies only for $(V/\sigma)^* > 1/3$ (Bender88)

18

# The revolution of IFS surveys




SAURON survey: deZeeuw+02
48 ETGs + 24 spirals

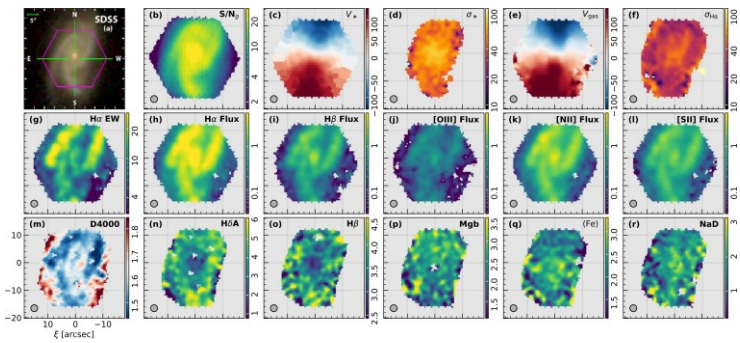
ATLAS$^{3D}$ survey: Cappellari+11
260 ETGs volume-limited

CALIFA survey: Sanchez+12
600 ETGs + spirals

19

# The race to larger IFS samples via multiplexing

- Multiplexed surveys
- SAMI 13 IFUs: Croom+12
  - 3068 galaxies observed
  - Final data release in 2021
- MaNGA 17 IFUs: Bundy+15
  - 10,000 galaxies observed
  - Final data release in 2021
- Hector: Bland-Hawthorn+15
  - 100,000 galaxies planned
  - Aims for end of the decade




MaNGA Data Analysis Pipeline products
(Westfall+19)

20

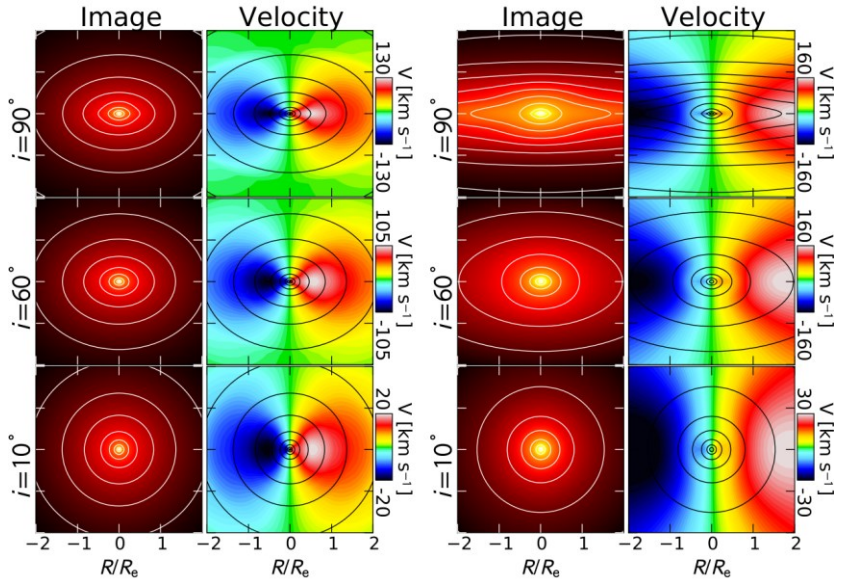
# Astrophysics C1
# Advanced stellar astrophysics and galaxies
# Lecture 11

**Michele Cappellari**

UNIVERSITY OF OXFORD

1

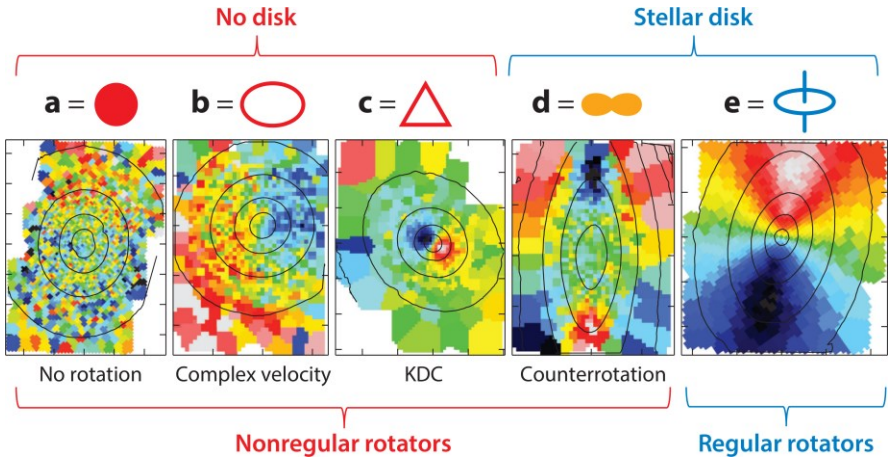
## Detect nearly face-on stellar disks




Cappellari-16 ARA&A

2

# Kinematic Morphology

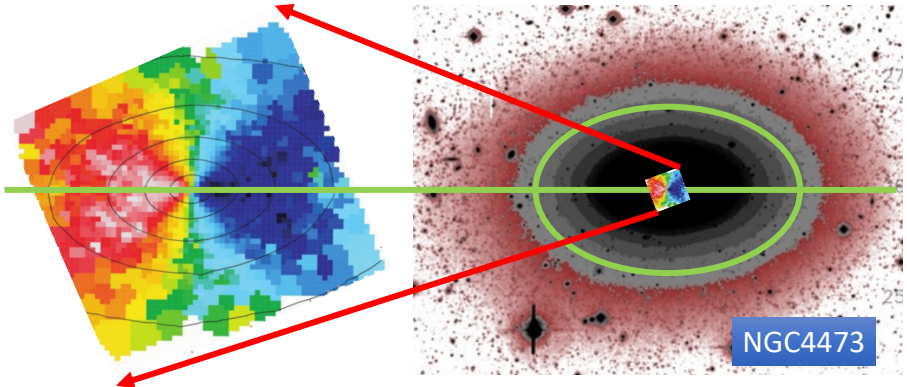



- Variety of kinematic maps
- But two major classes: non-regular/regular

(Cappellari-16 ARA&A)

3

# Measuring kinematical misalignment

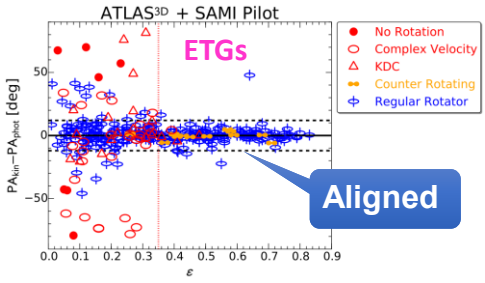



SAURON stellar velocity; MegaCAM image (Duc+15)

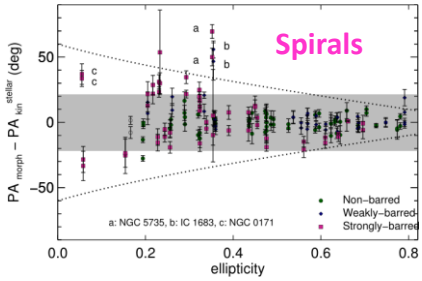
- $\mathrm{PA}_{\mathrm{kin}}(1R_e) \approx \mathrm{PA}_{\mathrm{phot}}(3R_e)$ (Krajnovic+11)
- Kinematics aligned with outer stellar halo
- Stellar halos consistent with axisymmetry

4

# Regular rotators/spirals are axisymmetric




(Krajnovic+11 + Fogarty+15)



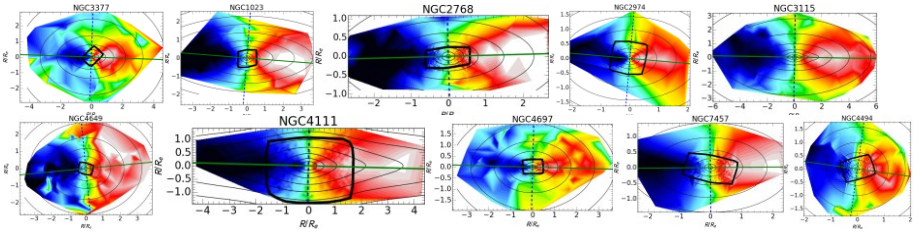

(Barrera-Ballesteros+14)

- 90% of all regular rotators aligned within $\approx 5°$
- Better aligned than spiral galaxies
- Only exceptions are bars and interactions
- Axisymmetric out to the stellar halo $\sim 3R_e$

5

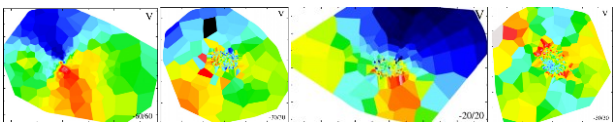
# ETGs misalignment at large radii

Regular rotators




Stellar kinematics from Arnold+14

Non-regular rotators

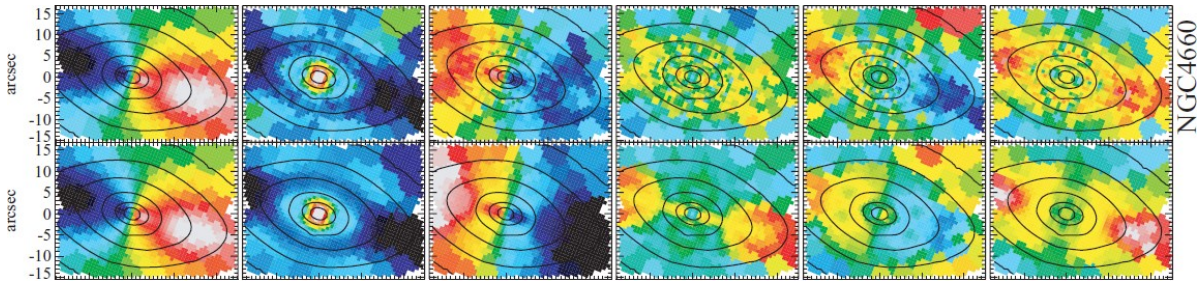





- SLUGGS survey: stellar kinematics to $\approx 4R_e$: Brodie+14
- **Regular rotators** remain aligned in the stellar halo
- **Non-regular rotators** remain misaligned (or non-rotating)

6

# Orbital distribution from IFU data

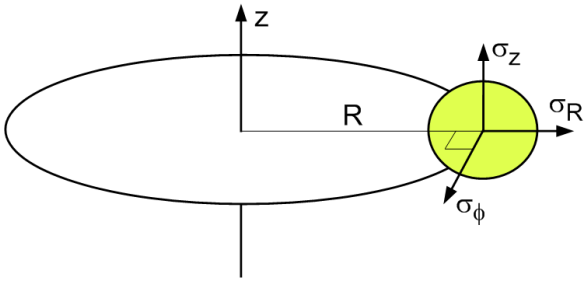



- Photometry reproduced in detail
- Fit full high-S/N LOSVD per Voronoi bin
- 3-dim data cube and 3-dim DF $= f(E, L_z, I_3)$
- Unique inversion from the data cube when the potential is known

Schwarzschild's models (Cappellari+07)

7

# Anisotropy and velocity ellipsoid

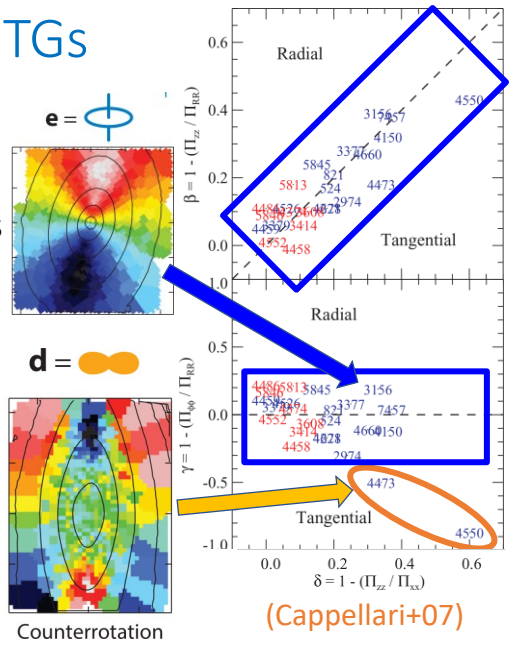



- $\beta = 1 - \frac{\sigma_z^2}{\sigma_R^2}; \gamma = 1 - \frac{\sigma_\phi^2}{\sigma_R^2}; \delta = 1 - \frac{2\sigma_z^2}{\sigma_R^2 + \sigma_\phi^2}$ (Cappellari+07)
- $\delta$ is measured by the (V/σ,ε) diagram (Binney78, 05)
- $\beta, \gamma$ require dynamical models
- $\sigma_R = \sigma_\phi \rightarrow (\delta = \beta;\ \gamma = 0)$: Oblate velocity ellipsoid

8

# Anisotropy of flattened ETGs

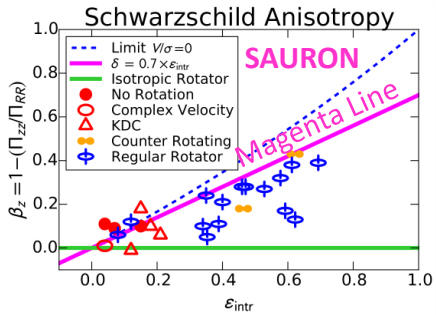
- Integral-field stellar kinematic data
- Schwarzschild's axisymmetric models
- Result: $\delta \approx \beta$ and $\gamma \approx 0$
- → average oblate velocity ellipsoid
- Exceptions: counter-rotating disks



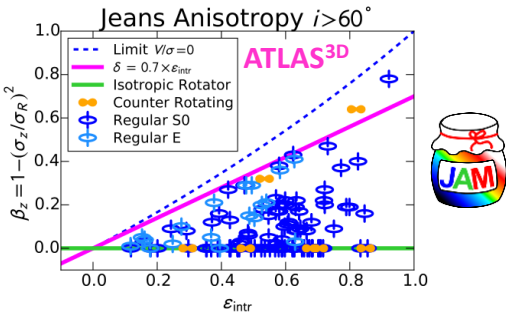

(Cappellari+07)

9

# Anisotropy depends on flattening




(Cappellari+07)

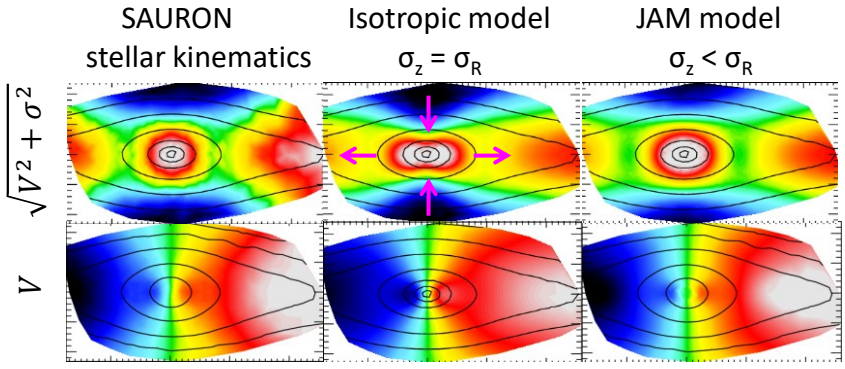



(Cappellari-16)

- Round galaxies isotropic (within $1R_e$)
- Flat galaxies can be anisotropic
- Maximum anisotropy depends on flattening

10

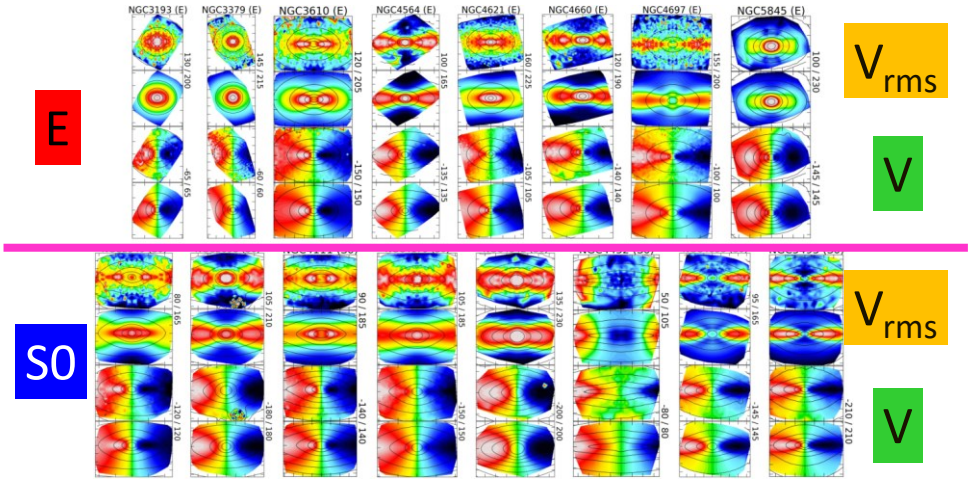
# Jeans Anisotropic Models




- Use Multi-Gaussian fit to images (Emsellem+94; Cappellari-02)
- Solve Jeans equations with cylindrically-aligned velocity ellipsoid
- Efficient Jeans solution with $\sigma_z \neq \sigma_R \neq \sigma_\phi$ (Cappellari-08)
- Just two parameters $(i, \sigma_z/\sigma_R)$ fit shape of both $V_{rms}$ and V!

11

# Regular kinematics highly predictable



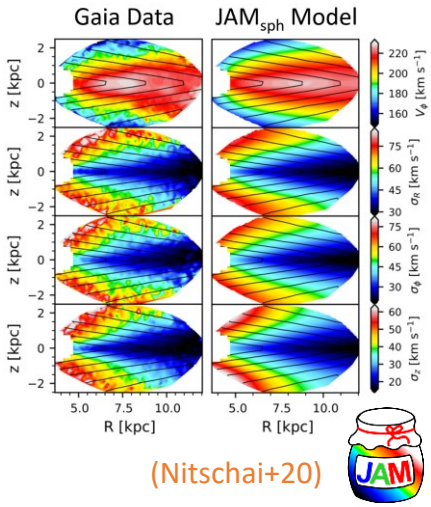

JAM models (Cappellari-08) of ATLAS$^{3D}$ kinematics

- Once accurate photometry is given
- Regular kinematics essentially "predicted" by $\beta_z = 1 - \sigma_z^2/\sigma_R^2$

12

# Milky Way dynamics like a fast rotator

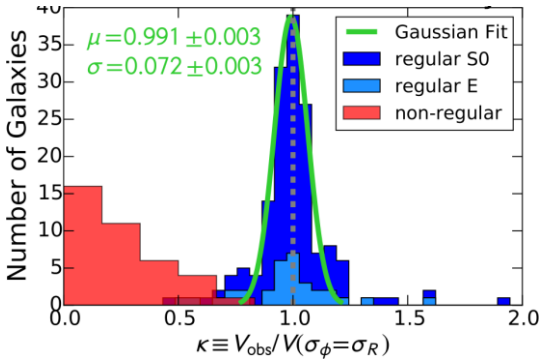
- Adopt best Milky Way stellar model (Juric+08)
- Take simple JAM model (Cappellari-08,20)
- Major difference: Gaia gives full 6-dim phase space coordinates $(x, y, z, v_x, v_y, v_z)$!
- No freedom/degeneracy in anisotropy
- Gaia DR2 kinematics naturally reproduced
- Milky Way spiral galaxy dynamically indistinguishable from ETGs fast rotators




(Nitschai+20)

13

# Stellar rotation dichotomy




Cappellari-16
ARA&A

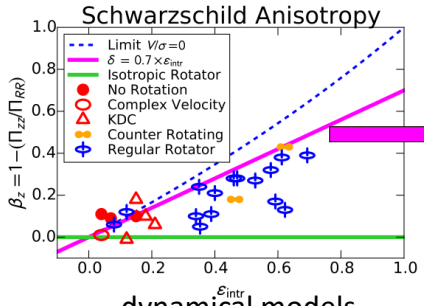
- Regular rotators have oblate velocity ellipsoid
  - Observed scatter of 7% including models errors!
  - Consistent distribution for both E and S0 galaxies
- Non-regular rotators follow different distribution

14

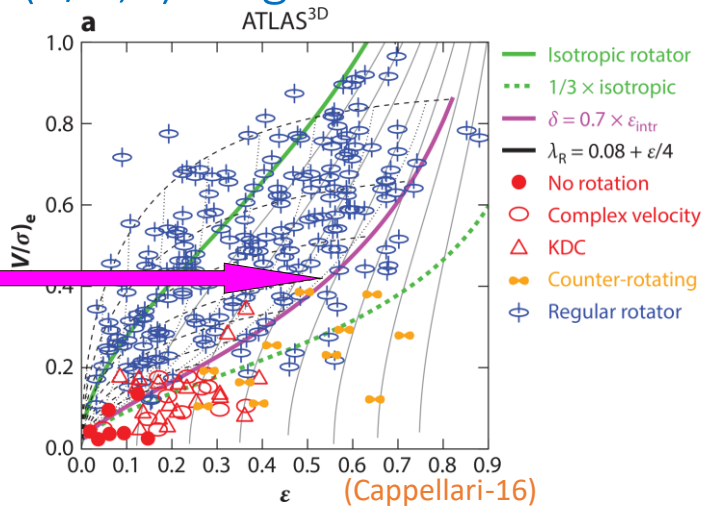
# Understanding the (V/σ,ε) diagram

Use integral-field kinematics

$$\left(\frac{V}{\sigma}\right)_e \equiv \frac{\langle V^2 \rangle}{\langle \sigma^2 \rangle}$$ (Binney 2005)




dynamical models (Cappellari+07)

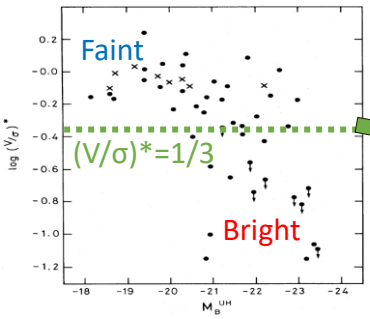



(Cappellari-16)

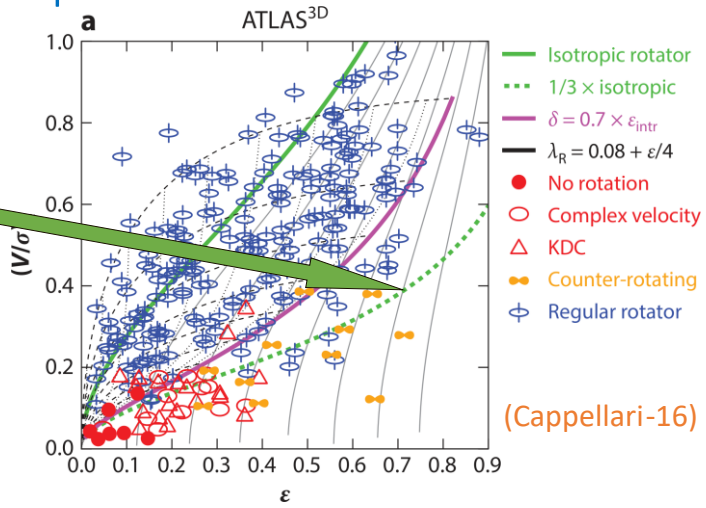
- (V/σ,ε) consistent with dynamical models
- Fast and slow rotators distinct on (V/σ,ε)

15

# Revisiting the (V/σ)* parameter




(Davies+83)

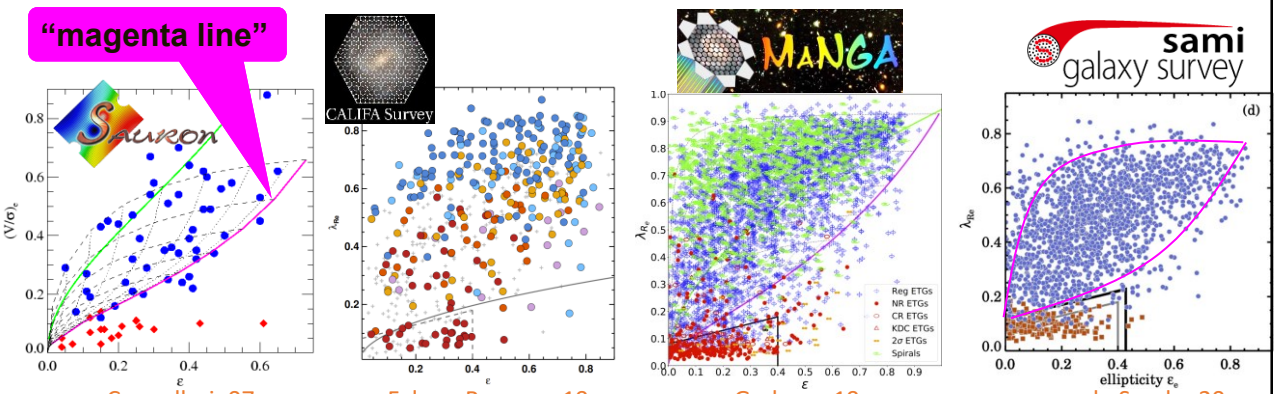



(Cappellari-16)

- Fast rotators: anisotropic oblate family
- Slow rotators: weakly triaxial and brighter (Emsellem+07; Cappellari+07)

16

# Improvements in kinematic studies

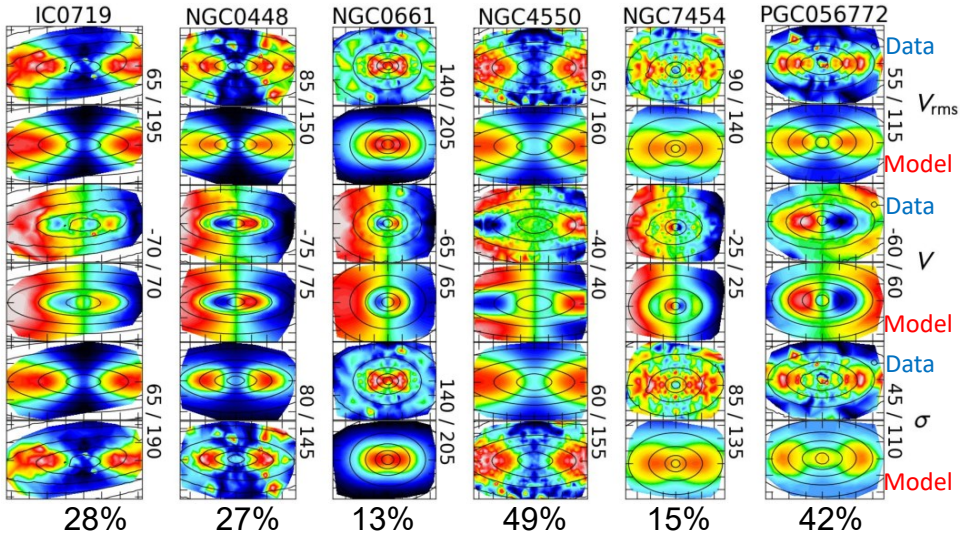



Cappellari+07 (V/σ by Binney-05) | Falcon-Barroso+19 | Graham+19 | van de Sande+20

- Sample increased by 2 orders of magnitude (since Emsellem+07)
- Initially, existence of classes and trends heavily debated

17

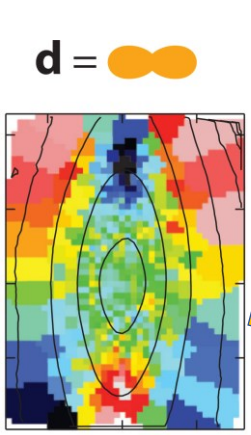
# Exception 1: counter-rotating disks



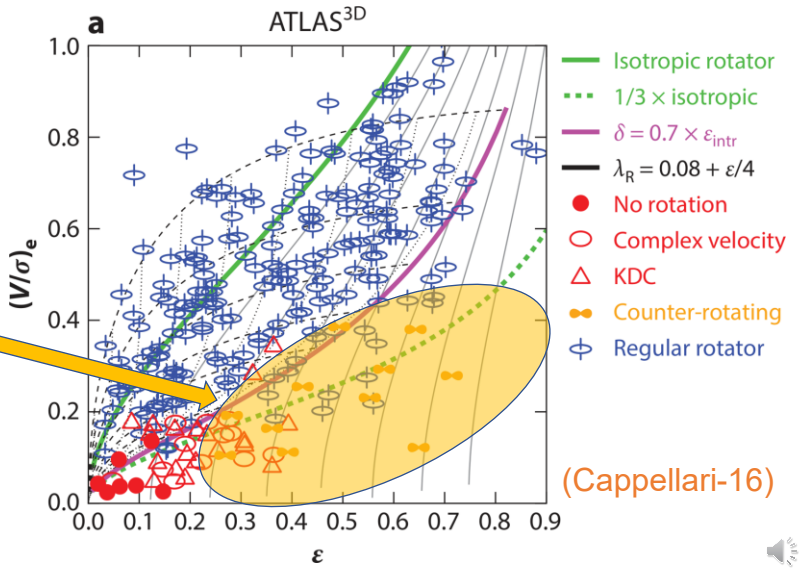

(Cappellari-16)

18

# Exception 1: counter-rotating disks



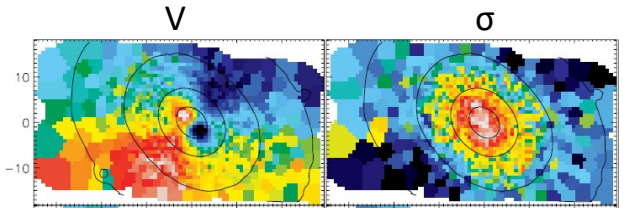

Counterrotation




(Cappellari-16)

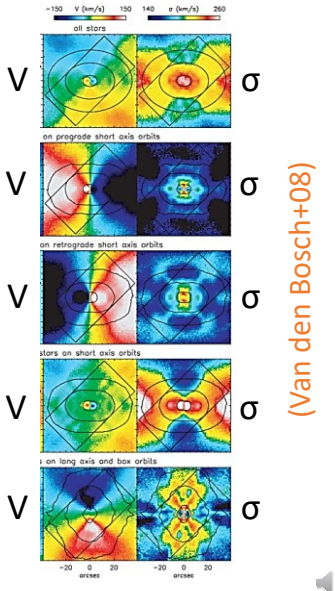
19

# Exception 2: KDCs in slow rotators




NGC4365 (Davies+01; vdB+08)

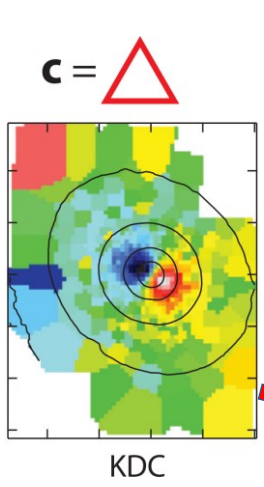
- Prototypical triaxial galaxy
- Orthogonal KDC (Wagner+88)
- KDC only “apparent”
- Cancellation of counter-rotating tube orbits (van den Bosch+08)

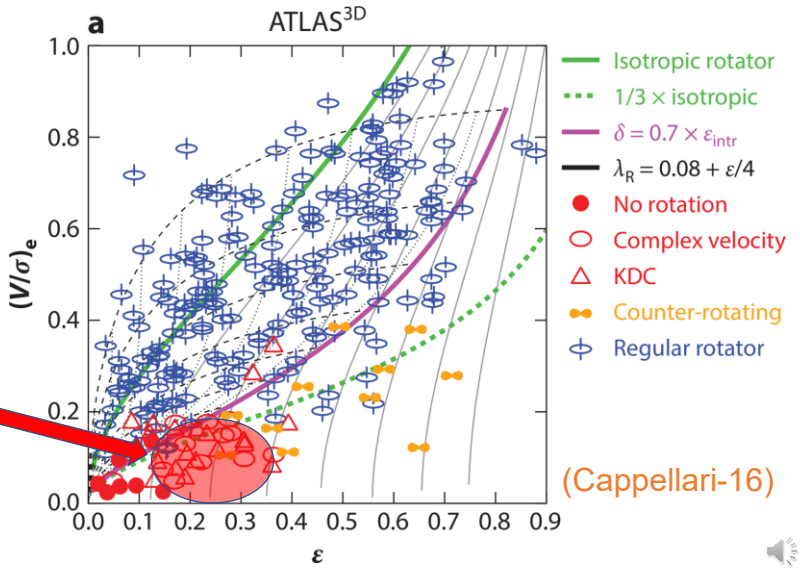



(Van den Bosch+08)

20

# Exception 2: KDCs in slow rotators

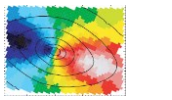



(Cappellari-16)

21

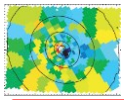
# Angular momentum vs Hubble's morphology



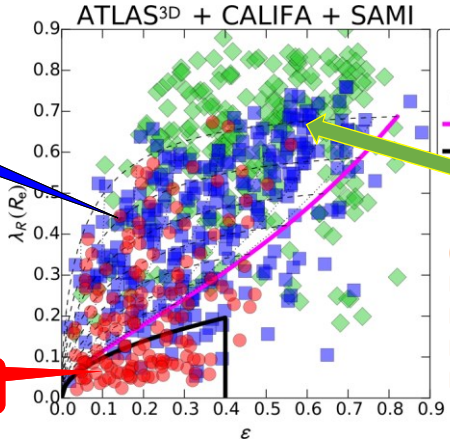
Fast ETGs

$$\lambda_R \equiv \frac{\langle R\,|V|\rangle}{\langle R\sqrt{V^2+\sigma^2}\rangle}$$

(Emsellem+07)



Slow ETGs





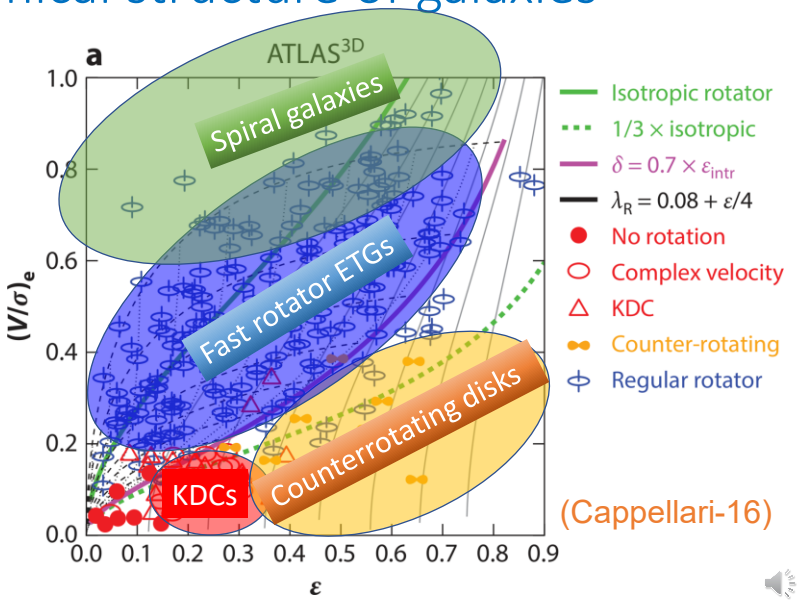

(Cappellari-16)
Data from:
Emsellem+11
Falcon-Barroso+15
Fogarty+15

- Trend angular momentum vs. morphology
- Explained by variation in bulge fraction
- Fast-rotator ETGs overlap with spiral galaxies
- 2/3 of ellipticals are fast rotators!

22

# Summary dynamical structure of galaxies

- Classic results revisited
- Most ETGs within 1Re: axisymmetric, randomly inclined, anisotropic, very homogeneous!
- Overlap with spiral galaxies sequence
- Exceptions
  - counter-rotating disks
  - "Apparent" KDCs in triaxial slow rotators




23

# Galaxy scaling relations

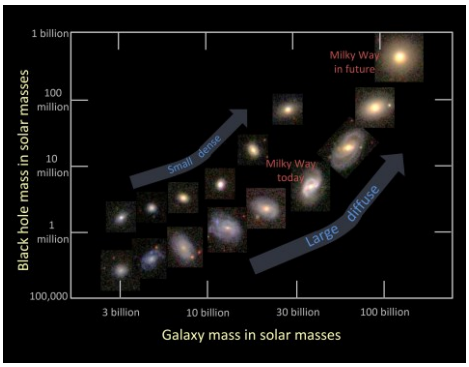
24

# Why studying dynamical scaling relations?

- Relate size, luminosity and kinematics
- Originally proposed as distance estimators
- Now ideal to compare galaxy formation models
- Constrain evolution of
  - Mass, radius, density, M/L

  → Dark matter

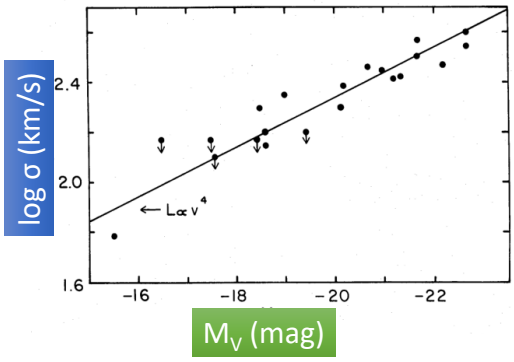
  → Stellar initial mass function



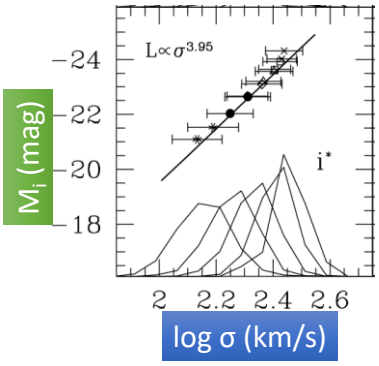

Credit: Sandra Faber/Sofia Quiros/SDSS

25

# Faber-Jackson relation $(L, \sigma)$




Faber-Jackson76

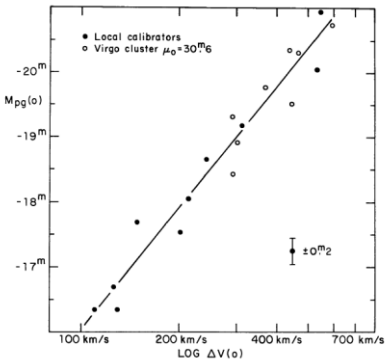



Bernardi+03 (9,000 SDSS)

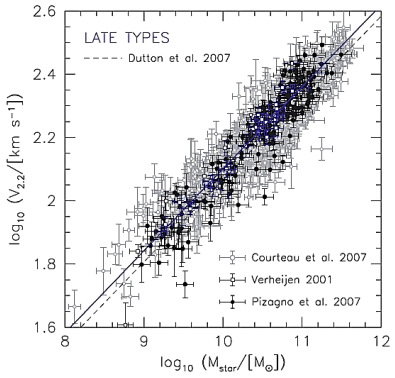
- $L \propto \sigma^4$ (Luminosity versus velocity dispersion)
- For elliptical galaxies
- Implies M/L increase with luminosity

26

# Tully-Fisher relation $(L, V_c^{\max})$




Tully+Fisher77

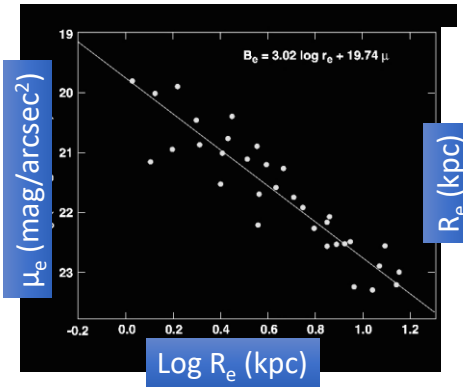



Dutton+11

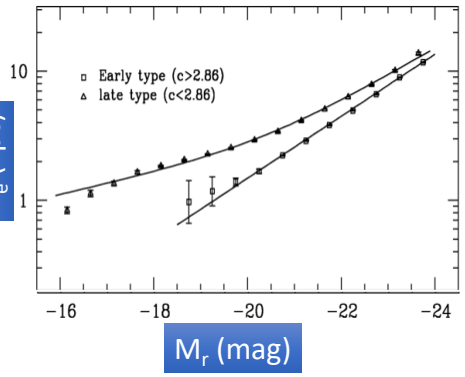
- Luminosity versus circular velocity $(V_c^{\max})$
- For spiral galaxies $L \propto V_c^4$

27

# Kormendy relation $(L, R_e)$




Kormendy77

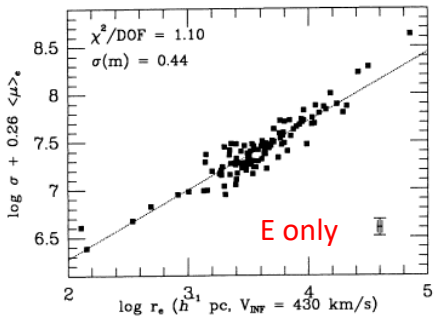



Shen+03 (140,000 SDSS)

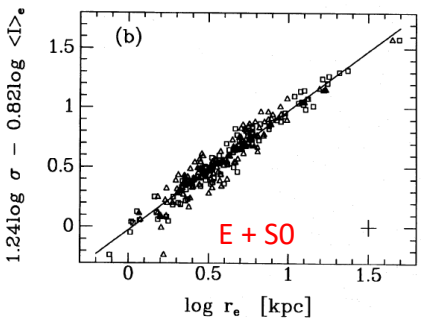
- Luminosity (or $\mu_e$) versus half-light radius $(R_e)$
- For early-type galaxies
- Popular at high-z as kinematics not needed

28

# Fundamental Plane $(L, \sigma, R_e)$




Dressler+87
Djorgovski+Davis87




Jorgensen+96

- Unifies luminosity, velocity dispersion and radius
- For both elliptical and lenticular galaxies

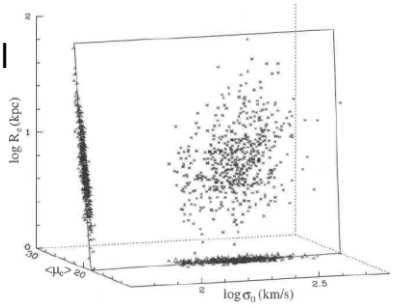
29

# Origin of Fundamental Plane

- For one galaxy in virial equilibrium
- $L \propto M \propto \sigma^2 R$
- If the M/L was the same for all galaxies
- And if the density/luminosity profile was universal
- $L = k\sigma^2 R$ with fixed $k$
- But observed exponents are not the virial ones
- $L \propto \sigma^{1.3} R^{0.8} \Rightarrow \lg L \approx 1.3 \lg \sigma_e + 0.8 \lg R_e + c$

→What produces 'tilt' in Fundamental Plane?
  - Genuine M/L variation? (dark matter/population IMF)
  - Non-homology? (surface brightness/kinematics)

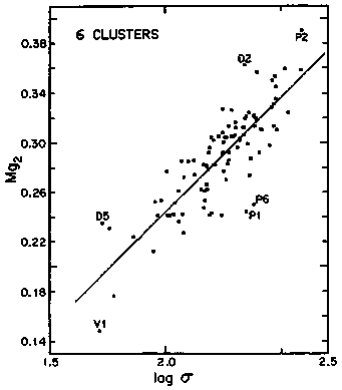
- Decades of debate…




30

# Variation of M/L in galaxies?

- Stellar population varies with mass
  - M/L increases with metallicity
  - M/L increases with age
    (Faber & Jackson 1976;
    Pahre, Djorgowski, & de Carvalho 1998)
- Variation in dark matter fraction
  - DM expected from formation scenario
  - DM fraction expected to vary
    (White & Rees 1978; Springel et al. 2005)

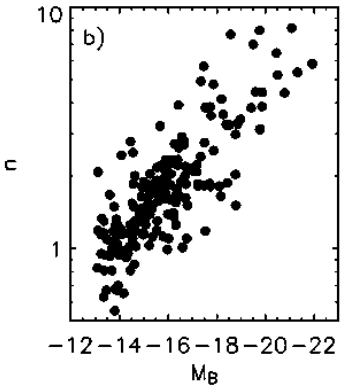



Dressler et al. (1987)

31

# Homology variation in galaxies?

- Light profile variation
  - Galaxy concentration increases with luminosity
  - σ increases with concentration
    (Caon, Capaccioli, & d'Onofrio 1993;
    Graham, Trujillo, & Caon 2001)
- Orbital distribution variation
  - Brighter galaxies rotate less
  - σ affected by rotation
  - Rotation not included in FP
    (Ciotti, Lanzoni, & Renzini 1996;
    Prugniel & Simien 1997)




Trujillo, Burkert, & Bell (2004)

32

# The solution: dynamical models

- Construct dynamical axisymmetric models
  - Include accurate 2-dim surface brightness
  - Fit 2-dim kinematics in detail
  - Explicitly include dark matter
- Derived M/L is unbiased
  - Free from homology and virial assumptions
  - Does it agree with virial predictions?
  - Does it explain the FP tilt?



33

# Astrophysics C1
# Advanced stellar astrophysics and galaxies
# Lecture 12

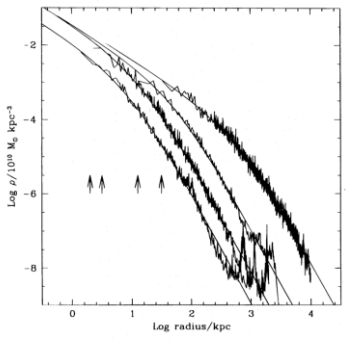
**Michele Cappellari**

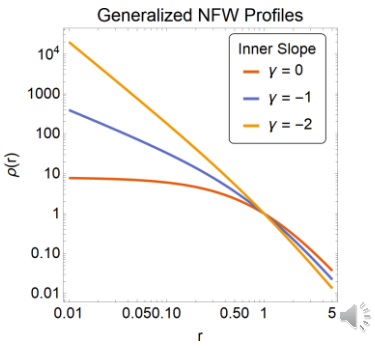
UNIVERSITY OF OXFORD

1

## Modelling dark-matter halos

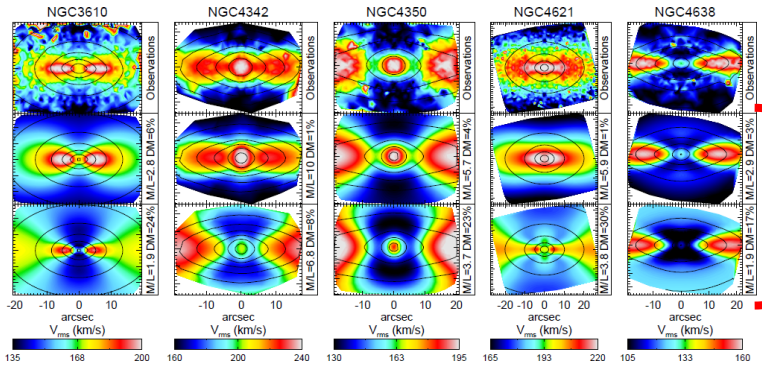
- Universal halo profiles in dark-matter-only simulations (Navarro, Frenk & White 1996; NFW)
- $\rho_{\rm NWF}(r) = \rho_s \left(\frac{r}{r_s}\right)^{-1} \left(\frac{1}{2} + \frac{1}{2}\frac{r}{r_s}\right)^{-2}$
- Inner density $r \ll r_s \Rightarrow \rho_{\rm NWF}(r) \propto r^{-1}$
- Outer density $r \gg r_s \Rightarrow \rho_{\rm NWF}(r) \propto r^{-3}$
- But baryons in simulations affect halo slope
- Safe to use generalized NFW halo profile (gNFW)
- $\rho_{\rm DM}(r) = \rho_s \left(\frac{r}{r_s}\right)^{\gamma} \left(\frac{1}{2} + \frac{1}{2}\frac{r}{r_s}\right)^{-\gamma-3}$
- Shape unknown: assume spherical




2

# Stellar and dark matter from Jeans models




$V_{rms} \equiv \sqrt{V^2 + \sigma^2}$

Data

← 1-6% dark matter

Models

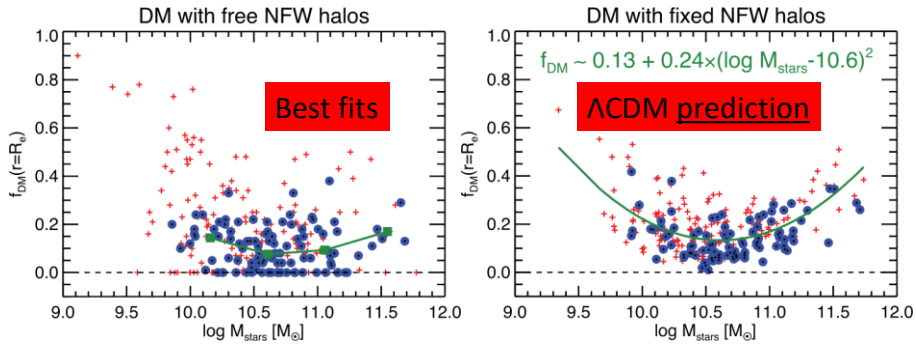
← 8-30% dark matter

(Cappellari+12a, Nature)

- With little dark matter $f_{DM}(r = R_e)$ Jeans models easily fit the data
- Models very sensitive to changing $f_{DM}(r = R_e)$
- Important caveat: if dark matter follows stars → complete degeneracy

3

# Small dark matter fractions $f_{DM}(R_e)$ in ETGs



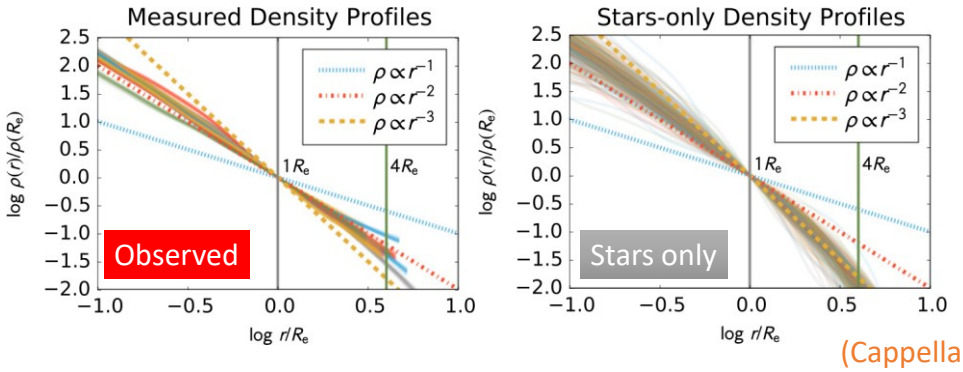

(Cappellari+13a)

- Best fitting median $f_{DM}(R_e) = 13\%$
- Fully consistent with ΛCDM prediction
  - Fixed-halo models fitted to real galaxies
  - Use NFW following $M_{200} - M_\star$ and $M_{200} - c_{200}$

(Moster+10, Behroozi+10, Guo+10)

4

# Nearly universal total-density profile in ETGs




(Cappellari 2015)

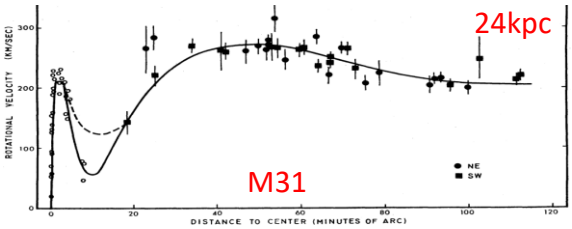
- Universal <u>total</u> mass profile to $4R_e$: $\rho_{tot} \propto r^{-2.2}$
- Observed rms scatter 0.11 in logarithmic slope
- Same as strong lensing studies near $R_e/2$ (Auger+10)
- Consistent with weak lensing stacks (Gavazzi+07)

5




6

# Spirals $V_c(r)$ from ionized gas




- Extended curves from ionized gas

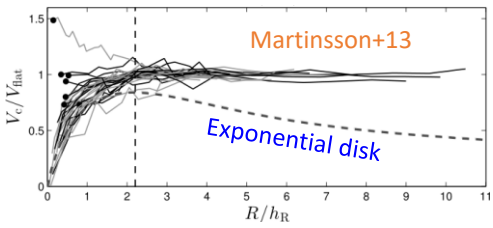
(Rubin-Ford70; Roberts-Whitehurst75; Rubin+80)

- Outer curves remain flat
- Limited to optical disk
- Initially no connection to dark matter made
- Need to estimate baryonic mass

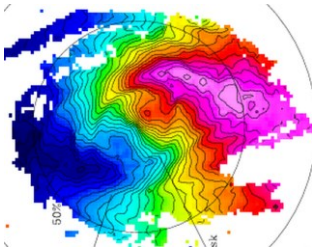


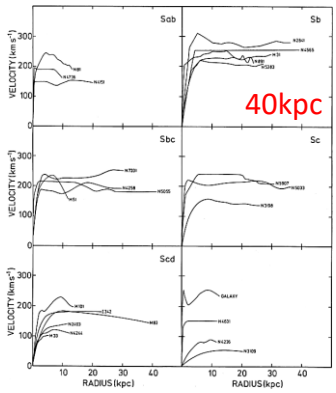

7

# Spirals $V_c(r)$ from neutral gas HI




- Radio HI observations
- Extend well beyond images
- Rotation curves still flat
- "it seems relatively certain that dark material is being detected" (Faber+Gallager79 ARA&A)



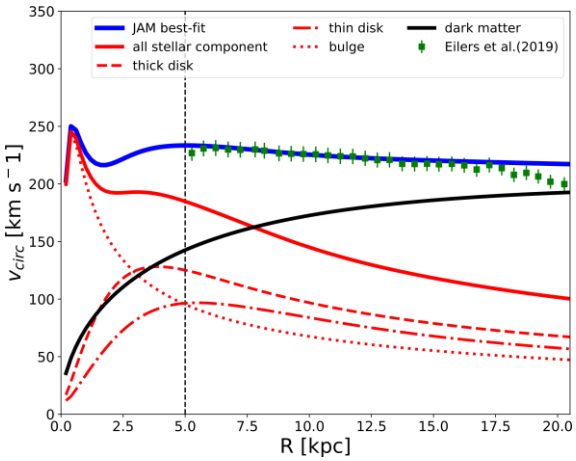

Bosma78 (PhD th. 540 cit.)

8

# Milky Way $V_c(r)$ from Gaia kinematics +



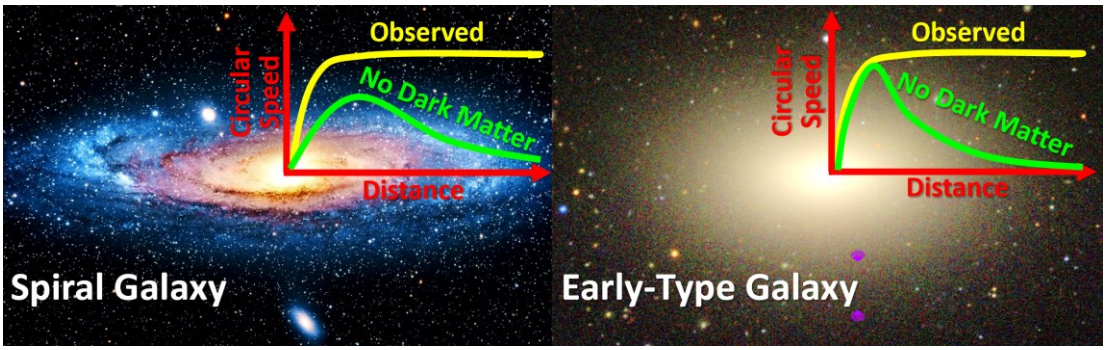

- Modelling Gaia stellar kinematics
- Axisymmetric Jeans models
- Circular velocity consistent with external galaxies
- Total density $\rho(r) \propto r^{-2.2}$ as ETGs




(Nitschai+21)

9

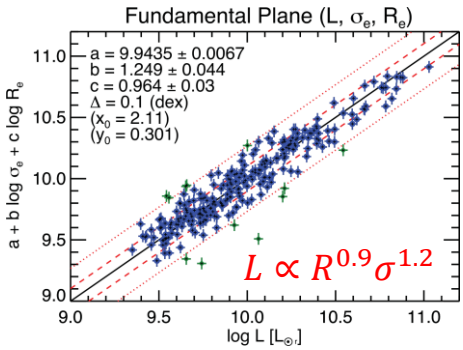
# The dark matter conspiracy

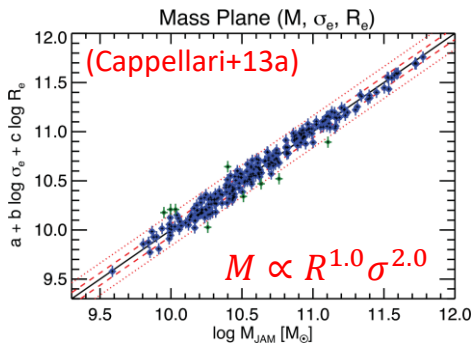



- Stellar density varies systematically in spirals and ETGs
- But total profiles remain nearly universal in massive galaxies ($\sigma_e \gtrsim 200$ km/s)
- Circular velocities $V_c(r)$ approximately flat
- This conspiracy may indicate a link in the dark and luminous matter evolution
- But many believe it may also indicate new physics beyond General Relativity

10

# ETGs Fundamental Plane = Virial equilibrium + M/L



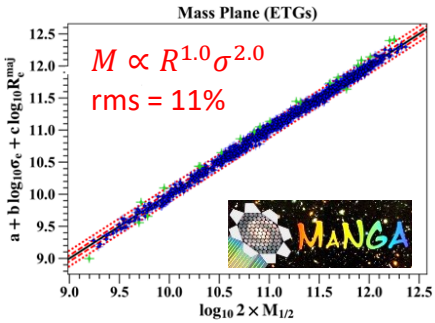



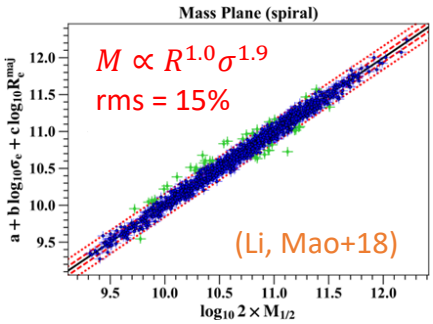

Luminosity → Mass

- MP has no intrinsic scatter: FP scatter due to population
- Follows virial prediction (as Cappellari+06, Bolton+08, Auger+10)
- But technique used for $R_e$ does matter!!!
- Galaxy formation encoded in inclined views of MP

11

# Spirals Mass Plane: No difference from ETGs



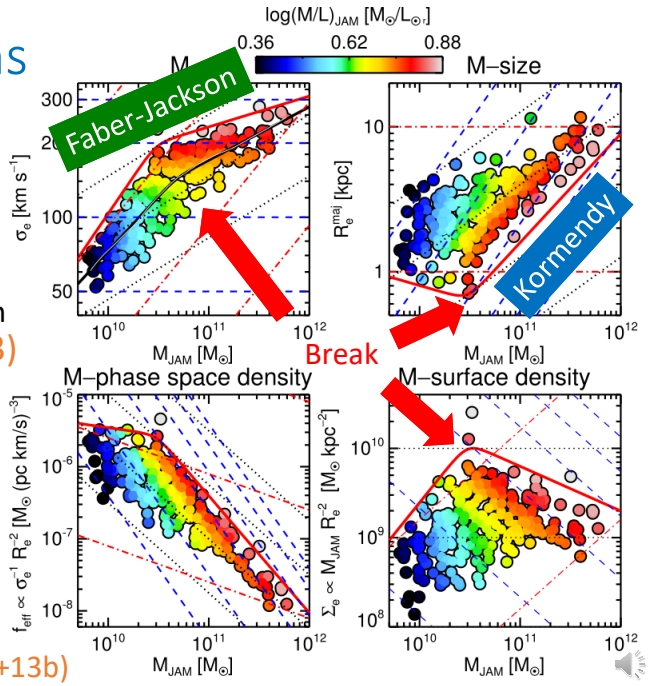




- 2000 ETGs + Spirals with integral-field kinematics
- Again: $\sigma_e$ measured within $1R_e$ → $\sigma_e \approx \langle V^2 + \sigma^2 \rangle^{1/2}$
- ETGs and Sp → "Generalized" scaling relation
- Same as for ETGs (i) No scatter (ii) Virial coefficients

12

# Mass Plane projections

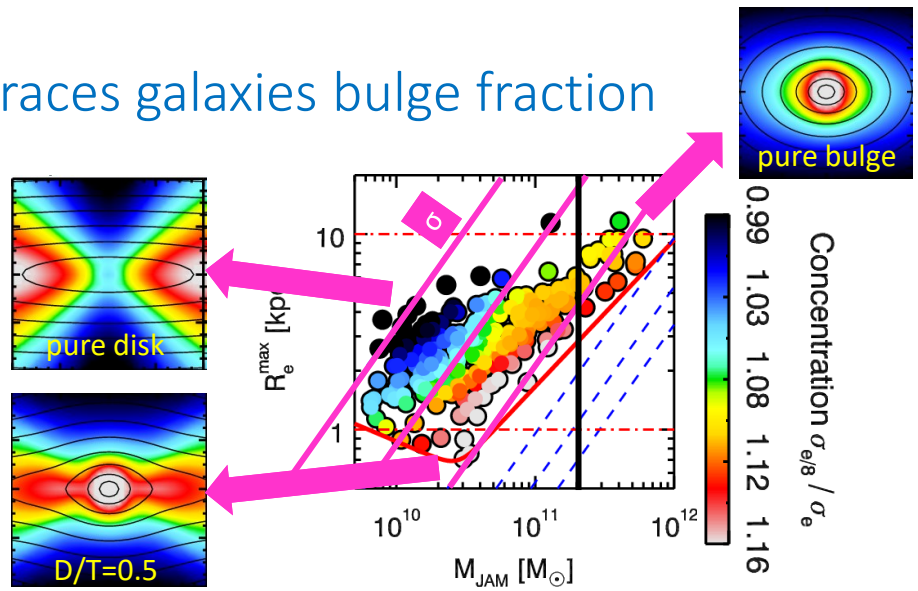
- All projections are equivalent
- They give the same general picture
- Mapped by virial equation $\mathrm{M} \propto R_e \sigma_e^2$
- Both M-$R_e$ and M-σ "relations" broken at $3 \times 10^{10} M_\odot$ (cfr. Kauffmann+03)
- $M \propto \sigma^{4.6}$ (large M)
- $M \propto \sigma^{2.2}$ (small M)




(Cappellari+13b)

13

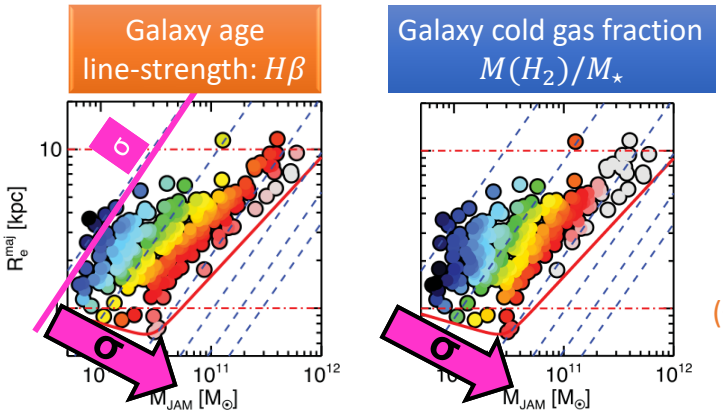
# $\sigma_e$ traces galaxies bulge fraction




- σ gradient $\equiv \sigma(\frac{R_e}{8})/\sigma(R_e)$ → bulge fraction

14

# Galaxy properties linked to bulge fraction ($\sigma_e$)

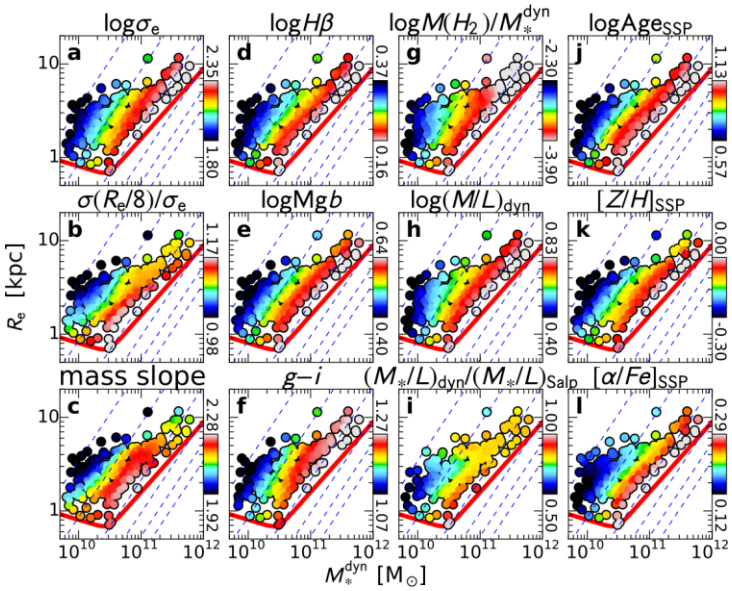



(Cappellari+13b)

- Galaxy parameters driven by $\sigma$ (not mass, Σ, Sersic-n)
- $\sigma_e$ traces bulge <u>mass</u> fraction

15

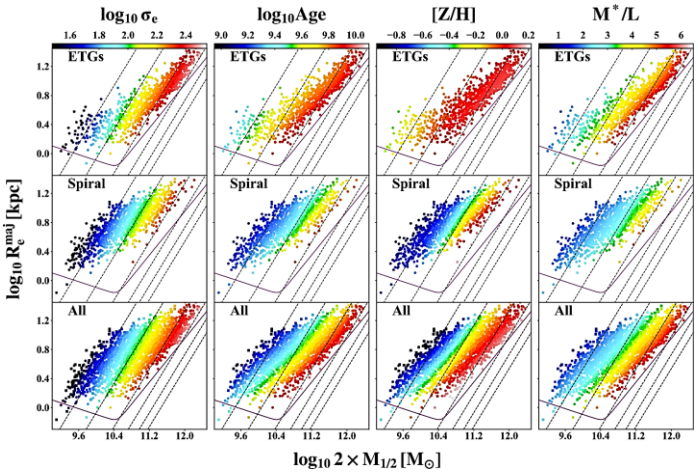
# Galaxy properties linked to bulge fraction




Cappellari-16 ARA&A

16

# Same trends for spirals and early-type galaxies





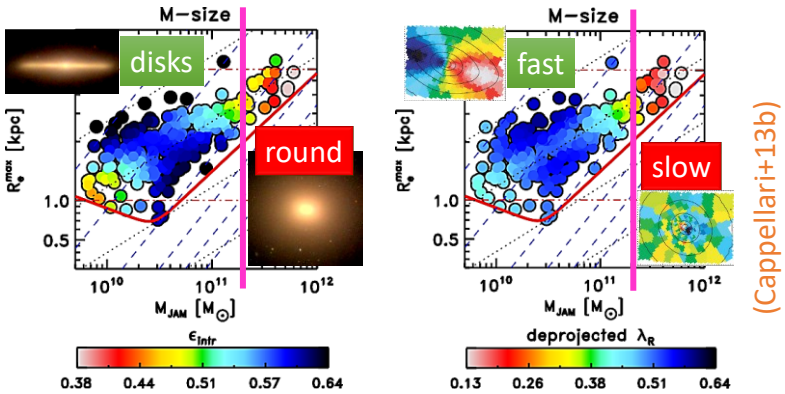


(Li, Mao+2018)

- Trends confirmed for much larger samples
- Valid for all morphological types

17

# But shape & rotation follow $M_\star$ not $\sigma_e$

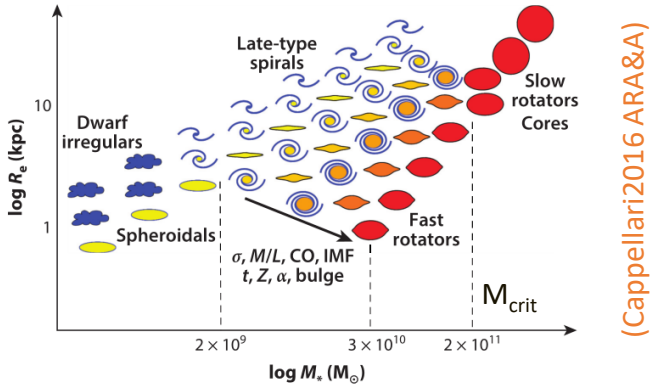



(Cappellari+13b)

- Characteristic galaxy stellar mass: $\mathrm{M_{crit}} \approx 2 \times 10^{11} \mathrm{M_\odot}$
- Spiral galaxies and fast rotators with low Sersic n dominate for $M_* \lesssim M_{\mathrm{crit}}$
- Slow rotator with central cores and high Sersic n when $M_* \gtrsim M_{\mathrm{crit}}$

18

# Summary of galaxy structure



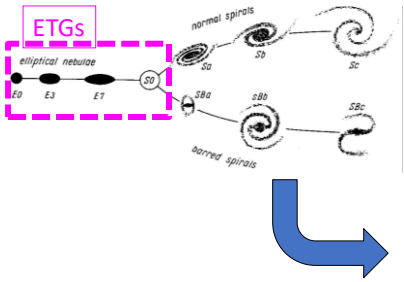

(Cappellari2016 ARA&A)

- Bulge fraction linked to quenching of star formation
  (see Cappellari+11b; Kauffmann+12; Bell+12; Cheung+12; Fang+12)
- Three characteristic galaxy stellar masses
  (cfr. Davies+83; Faber+97; Kauffmann+03; van der Wel+09; Geha+12)

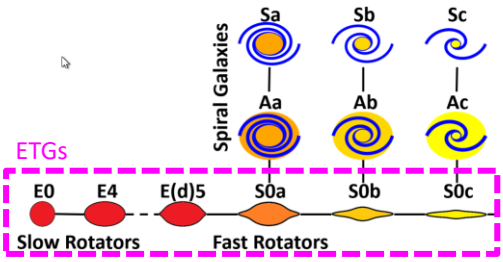
19

# Revisiting galaxy classification with kinematics

Hubble (1935)




Cappellari+11b



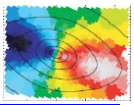

- Fast rotators: parallel sequence to spirals
  (see Spitzer+Baade51; van den Bergh76; Kormendy & Bender 2012)
- Not misclassified spirals!
- ETGs generally not spheroidal but disk-like
- Hubble diagram does not properly describe ETGs

20

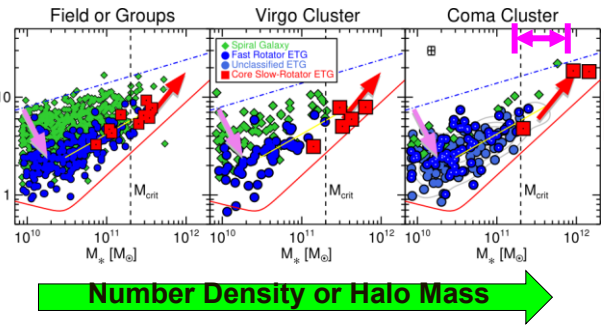
# Two channels of galaxy evolution

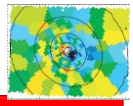


spiral



fast ETG



slow ETG

Coma dark halo:
$M \approx 1.4 \times 10^{15}\ M_\odot$
(Lokas+Mamon03)

$\Delta \log \Sigma_3 \sim 3$
increase in number density

Kinematic classification from IFS (Cappellari-13)

**Spirals → Fast rotators**

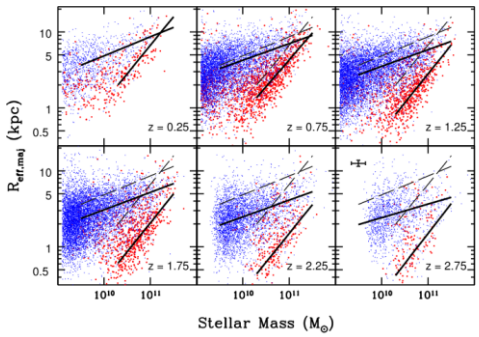
- Slow mass increase
- Environment quenching
- Bulge quenching

**Core slow rotators →**

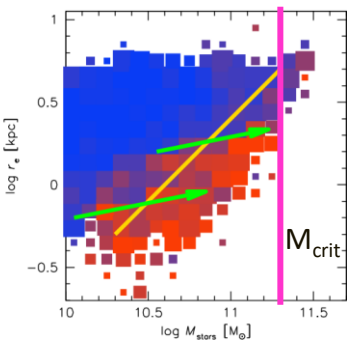
- Mass growth $M \propto R_e$
- Halo quenching
- Luminosity gap

21

# Mass-size evolution with redshift




(van der Wel+14)

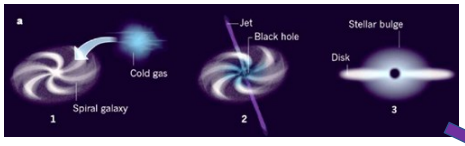



(van Dokkum+15)

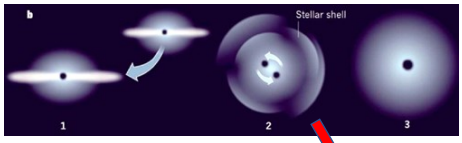
- Evolution can be traced out to $z \sim 3$
- Also indicates two channels of formation
  - Slow growth dominated by star formation
  - Rapid growth by mergers

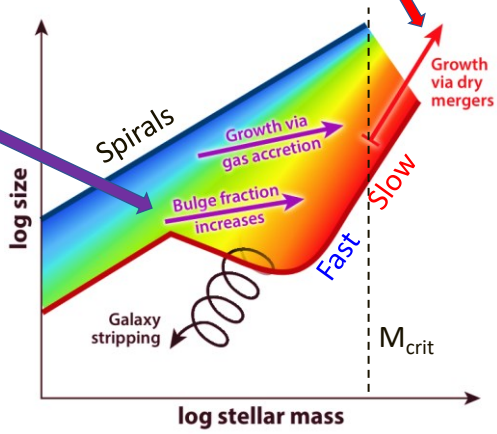
22

# Summary of galaxy evolution




Cappellari-11 Nature




- Two channels of galaxy formation
- Also explains observed black hole scaling relations (e.g. Kormendy-Ho 13, Grahm-Scott13, van den Bosch-16)
- But galaxies do not follow both in sequence!

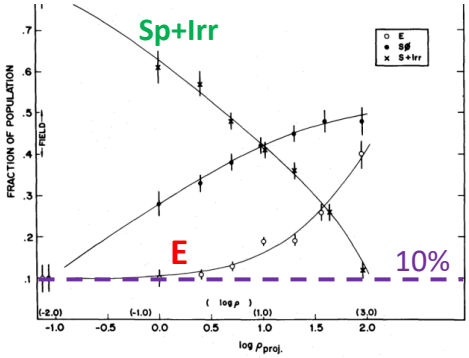
(Cappellari-16 ARA&A)

23

# Environmental dependency

24

# Morphology-density ($T - \Sigma$) relation

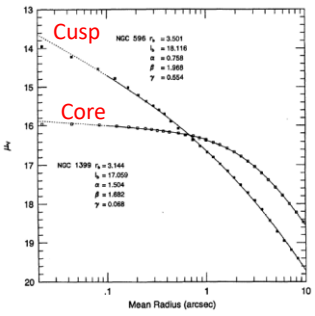



(Dressler-80)

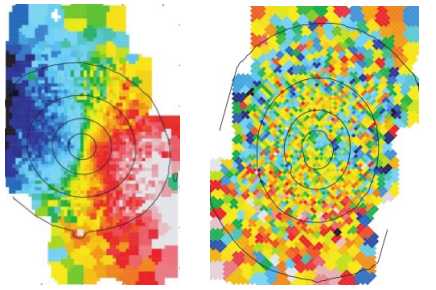
- Morphology *T* dependence on num. dens. $\Sigma$
- Spirals transforms into E+S0 in clusters
- But why 10% of E still present in the field?

25

# Core + slow rotator = dry merger



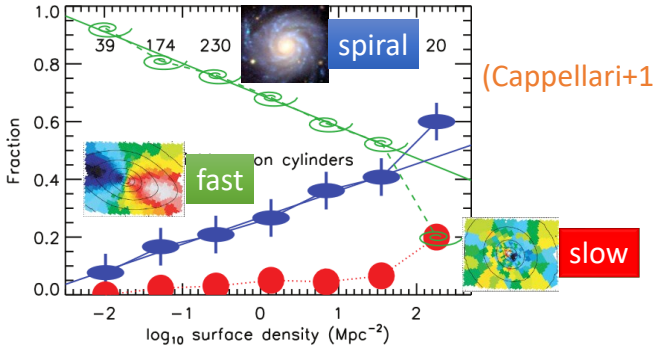

Lauer et al. 1995




- Core ≈ dry merger (e.g. Kormendy+09)
- Slow rotator ≈ dry merger
- But exceptions exist (Lauer+13; Krajnovic+13)
- Core + slow rotator = dry merger

26

# Evolutionary channel: Spirals → fast rotators

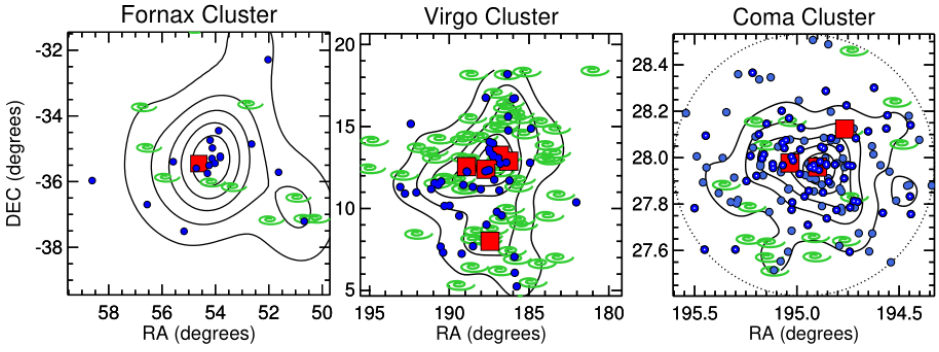



(Cappellari+11b)

- Opposite trend spirals/fast rotators
- But slow rotators nearly absent in the field!
- Field Es were misclassified S0s
- Sharp rise of slow rotators in cluster

27

# Core slow rotators in cluster centres

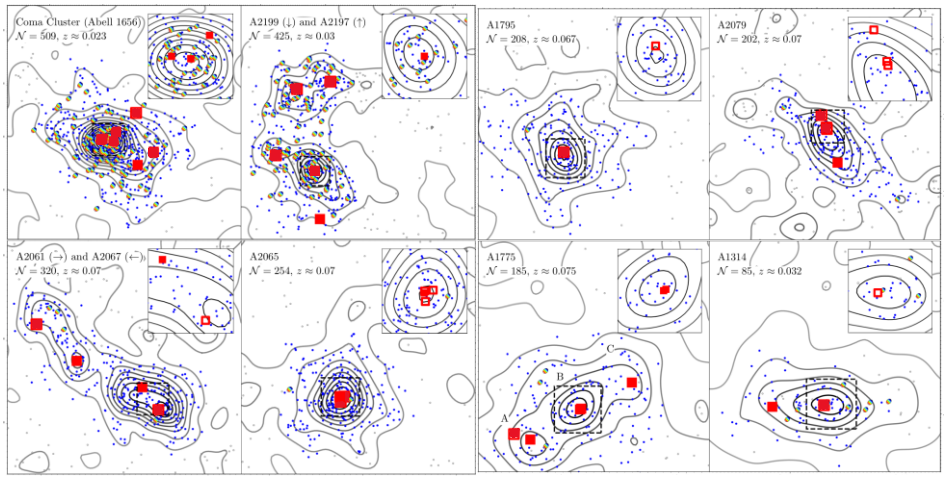



(Scott+14) (Cappellari 2013 ApJL)

- Strong decrease of spirals in Coma
- Strong increase of fast rotators
- But less core slow rotators in Coma

28

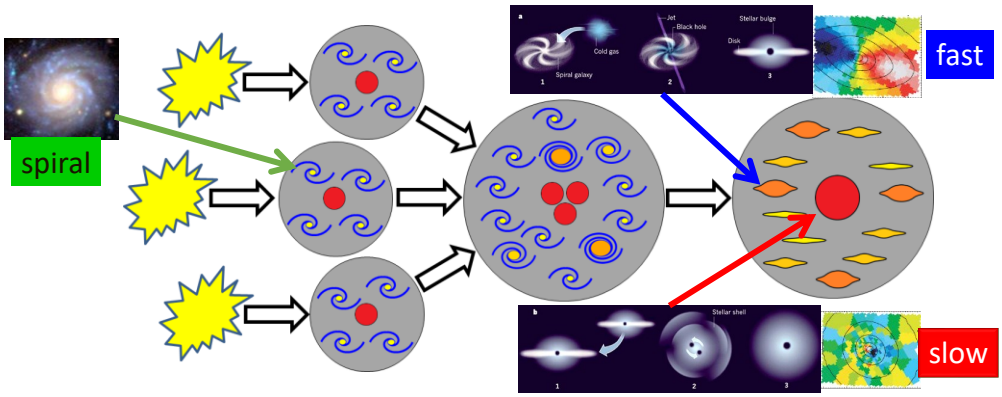
# Slow rotators in MaNGA clusters: maps




- 10 massive Abell clusters (Graham+19)
- Slow rotators trace sub-clusters density peaks

29

# Hierarchical morphology evolution




**Spirals to fast rotators ETGs**

- Generally satellites
- Quenched by environment
- Or by internal processes
- Bulge grows with quenching

**Core slow rotators**

- Generally near halo centre
- Sink by dynamical friction
- Mass grows by dry mergers
- Halo/BH quenching

30